JOURNAL OF NEUROPHYSIOLOGY
Vol. 64, No. 5, November 1990. *Printed in U.S.A.*

# Components of Field Potentials Evoked by White Matter Stimulation in Isolated Slices of Primary Visual Cortex: Spatial Distributions and Synaptic Order

RONALD B. LANGDON AND MRIGANKA SUR
*Department of Brain and Cognitive Sciences, Massachusetts Institute of Technology, Cambridge, Massachusetts 02139*

## SUMMARY AND CONCLUSIONS

*1.* We have recorded profiles of the spatial distributions of extracellular field potentials in transverse slices of rat primary visual cortex. Responses were evoked by electrical stimulation near the white matter/layer VI border and sampled from layers I to V along the radial axis orthogonal to the laminae and intersecting the stimulation site ("on-beam" recording). To assess the activity of "horizontal" connections, we also recorded profiles along axes parallel to the cortical lamination ("off-beam" recording), usually in layer III. Overall, our goal was to extend understanding of the physiology and organization of neocortical circuitry and to provide a basis for comparisons of data from different experiments and experimenters when neocortical field potentials are used in studies of plasticity and pharmacology.

*2.* Responses were highly specific with respect to the cortical layers. We distinguish four major components: two kinds of population spike ("S1" and "S2") and two slower waveforms ("W1" and "W2"). The latter appear to represent flow of current in apical dendrites of the supragranular layers. Component W1, the earliest slow component, is a synaptically driven field potential dipole that is positive in layer I and negative in layer II. Based on estimates of current source densities (CSDs), we attribute this to entry of depolarizing current into dendrites and/or cell somata in layer II, ascending intradendritic current, and passive depolarization of inactive dendritic membrane in layer I. Component W1 rises during the 20 ms after stimulation and falls during the 50–100 ms thereafter. Component W2 is also positive in layer I but maximally negative in layer III. It rises for ~100 ms after stimulation and decays during the following 400–800 ms.

*3.* Component S1 does not depend on synaptic transmission because it persists during the application of glutamate receptor antagonists or medium that is low in $Ca^{2+}$. This component is largest in layer III, radial to the site of stimulation. There, it is a negative deflection, typically 1–2 mV in amplitude and lasting roughly 2 ms, with a latency to peak between 2 and 4.5 ms. Component S1 is most likely a population spike due to synchronized firing of cell somata activated antidromically via unmyelinated efferent axons.

*4.* Component S2 is a short (<20 ms) burst of population spikes specifically in layer III. Individual S2 spikes closely resemble S1 spikes, and we propose that the same neuronal population generates both. However, S2 spikes require glutamatergic synaptic transmission. Also, S2 spikes are observed both on-beam and off-beam. During S2 spike bursts, the interspike interval (2.5–4.5 ms) remains nearly constant. These population bursts are tightly phase-locked to the stimulation, and burst amplitudes are graded with respect to stimulus strength.

*5.* Depth profiles sampled off beam include components resembling S2, W1, and W2, as defined on-beam. However, short-latency (5–9 ms) S2 spikes occur within 400 μm of on-beam, exclusively. The extent of horizontal spread of responses varies between preparations, ranging up to 1.8 mm. Response latencies increase by 10–15 ms for each millimeter of horizontal displacement.

*6.* We propose that firing by layer III pyramidal cells is driven and synchronized by short-latency, excitatory neurotransmission mediated by recurrent collaterals. During normal function in vivo, layer III pyramids may respond to specific patterns of visual stimulation by firing as ensembles. Our data imply that most members of such an ensemble would be situated within 300 to 400 μm of each other.

## INTRODUCTION

The mammalian visual cortex is a region of brain that has been studied intensively, both because of interest in how it processes visual information and also in the hope that it may serve as a model for neocortex in general. We now have a considerable body of data concerning the role of visual activity in the development of thalamic afferents to this region (reviews by Frégnac and Imbert 1984; Sherman and Spear 1982), the constituent neurons of visual cortex, their projections, and patterns of firing by single units in response to specific patterns of visual stimulation (reviews by Gilbert 1983; Hubel 1982; Jones 1984, 1988; Lund 1981; Peters 1984). In contrast, our understanding of field potentials in visual neocortex (and in neocortex in general) has remained at a primitive level.

In a number of other regions of vertebrate nervous system, analysis of field potentials evoked by bulk stimulation of afferents or efferents has proven very useful, principally for two reasons. *1)* Field potentials are generated by the concerted activity of populations of neuronal elements. The amplitude of a field potential may thus provide useful information concerning the number of neurons firing in response to stimulation (Andersen et al. 1971) or the average strength of subthreshold postsynaptic currents evoked in the dendrites of a particular neuronal population. *2)* Under certain conditions, analysis of spatial distributions of field potentials may define relationships between anatomic location and the entry or exit of current into or from populations of neurons (Lorente de Nó 1947; Mitzdorf 1985; Nicholson and Freeman 1975). Moreover, the time course of a field potential may reveal the time required for the passive equalization of intracellular potential within a neuronal population (Langdon et al. 1988b). In no small part due to pioneering investigations by Andersen and co-

workers (1971, 1978, 1980), field potentials have played a major role in studies of pharmacology, synaptic organization, and plasticity in the rodent hippocampus. A partial list of other brain regions where this technique has been useful might include mammalian olfactory bulb (Rall and Shepherd 1968), the optic tectum of "lower" vertebrates (Freeman et al. 1980; Langdon and Freeman 1987; Langdon et al. 1988b), cerebellum (Nicholson and Llinas 1971), prepyriform cortex (Haberly and Shepherd 1973; Richards and Sercombe 1970), as well as early investigation of the neuromuscular junction (Eccles et al. 1941).

Although previous studies have described field potentials from various regions of rodent and cat neocortex, including a few specifically from primary visual cortex (Bode-Greuel et al. 1987; Hamasaki et al. 1987; Kimura et al. 1989; Komatsu et al. 1988; Mitzdorf 1985; Mitzdorf and Singer 1978, 1980; Perkins and Teyler 1988; Yamamoto et al. 1989), much has remained uncertain concerning the identity of evoked components and the neuronal activities that generate them. We present here an analysis of the components of field potentials evoked in rat visual cortex by electrical stimulation near the border between layer VI and the white matter. In our study we have combined the following experimental manipulations: *1*) the study of in vitro slices, *2*) pharmacologic isolation of nonsynaptic response components from those that are synaptically driven, *3*) focus on area 17, *4*) systematic study of the distribution of responses in all three spatial dimensions, *5*) careful correlation of recorded activity with identified cortical laminae, and *6*) estimates of current source and sink density distributions where appropriate. We performed our experiments in vitro because this allows greater control over the composition of the extracellular medium, the ability to directly visualize the placement of electrodes, and more favorable conditions for making intracellular recordings in future experiments. We chose to use rats based on a combination of scientific and logistic considerations. Visual responses of single units in area 17 have been studied much more extensively in cats and primates, but the major aspects of cell responses are similar in rodents (Burne et al. 1984; Métin et al. 1988; Peters 1984), as is the general pattern of interlaminar connections (Burkhalter 1989; Parnavelas et al. 1977). Moreover, this study was intended to investigate features of the intrinsic microcircuitry and extrinsic connectivity of visual cortex, rather than to explain specific aspects of visual response. We also wished to examine variability in responses and identify those aspects of the field potential that are the most reliably elicited. We therefore chose to build up an extensive data base from a large number of experiments with rat brain, rather than a smaller number of experiments with slices from cats (or primates).

Our new data include response components that generally bear resemblance to those in previous reports, but our more detailed findings lead to novel interpretations concerning the underlying cellular events. In particular, our data imply that local excitatory interactions are of special importance in layer III.

Portions of these data and conclusions have been previously presented in two abstracts (Langdon et al. 1988a, 1989).

## METHODS

### *Preparation and maintenance of slices*

Our "normal" slice medium was a solution composed of the following (in mM): 114 NaCl, 3 KCl, 2.5 $CaCl_2$, 1.2 $MgCl_2$, 1.2 $Na_2SO_4$, 10 D-glucose, 0.001 glycine, 10 *N*-2-hydroxyethylpiperazine-*N'*-2-ethanesulfonic acid (HEPES), 0.01 phenol red, 25 $NaHCO_2$, 1 sodium phosphate buffer (pH 7.0), and sufficient (~2.5 mM) HCl to bring pH to 7.4 when bubbled with 95% $O_2$-5% $CO_2$. To make "$Ca^{2+}$-free" medium, $MgCl_2$ was substituted for $CaCl_2$ (increasing the $[Mg^{2+}]$ from 1.2 to 3.7 mM). Cortical slices were prepared following conventional procedures (Alger et al. 1984) from 46 albino rats (Charles River) weighing 250–400 g. In brief, animals were deeply anesthetized by intramuscular injection of ketamine HCl (100 mg/kg) and acepromazine maleate (10 mg/kg). Lidocaine HCl (2%) was applied to the ear canals and wound margins. With the animal held in a stereotaxic apparatus, the occipital half of the left cortical hemisphere was exposed. The animal was exsanguinated by cardiac puncture, and a block of brain that included primary visual cortex was immediately removed and transferred to cold (4–8°C) slice medium. Still submerged, the block was sliced into 500-$\mu$m-thick coronal sections with a Vibratome (Oxford). These were suspended until use on nylon nets in a beaker of vigorously bubbled slice medium at room temperature.

We used a submersion-type slice chamber with a jet of $O_2/CO_2$ directed onto the surface of the fluid in the chamber (maintained at 33°C). Besides its role in physiological maintenance, the jet provided a slow swirling of the medium, which probably improved equilibration of drug concentrations during solution changes. In most experiments, slices rested on (from top to bottom) one sheet of lens paper, one layer of fine nylon netting (bridal veil), and a block of Sylgard. The slice was held submerged by a layer of nylon netting weighted with pieces of platinum wire. Based on the field-potential data, each slice was viable through its entire thickness (see below), and viability through time was excellent. Responses were studied between 2 and 12 h after death of the animal, during which there was no apparent deterioration of responses. In earlier experiments in which slices were laid directly onto the chamber floor, response amplitudes were generally smaller, and large potentials occurred only in the 300 $\mu$m nearest the upward face.

### *Definition of terms and anatomic locations*

We refer to displacement orthogonal to the pial surface as "radial." "Depth" refers to distance from the pial surface. A "depth profile" is an array of responses sampled at a series of depths, usually separated by 100 $\mu$m. The "*z*-axis" is the line along which a depth profile is sampled (Fig. 1*A*). Our usage of some anatomic terms differs from their standard meanings for intact brain. "Horizontal" refers to displacement within the cortex remaining at the same depth. The direction of horizontal movement that (obliquely) approaches the midline is called "medial"; the opposite direction is "lateral." The mediolateral dimension, thus defined, is called the "*x*-axis" (Fig. 1*A*). A "horizontal profile" is an array of responses sampled along the *x*-axis (while remaining at the same depth). The "*y*-axis" is the dimension that crosses the plane of the slice (Fig. 1*B*). Independent of synaptic transmission, there was conduction of impulses along the *z*-axis from the site of stimulation toward the pia (see RESULTS). We refer to this path of "direct" conduction as "on-beam." The rest of the cortex was "off-beam."

Locations of our recordings are based on the data of Zilles and co-workers (Zilles 1984; Zilles et al. 1985) and the atlas of Paxinos and Watson (1986). We use the term "area 17" as synonymous with their "Oc1," designating primary visual cortex. Zilles and

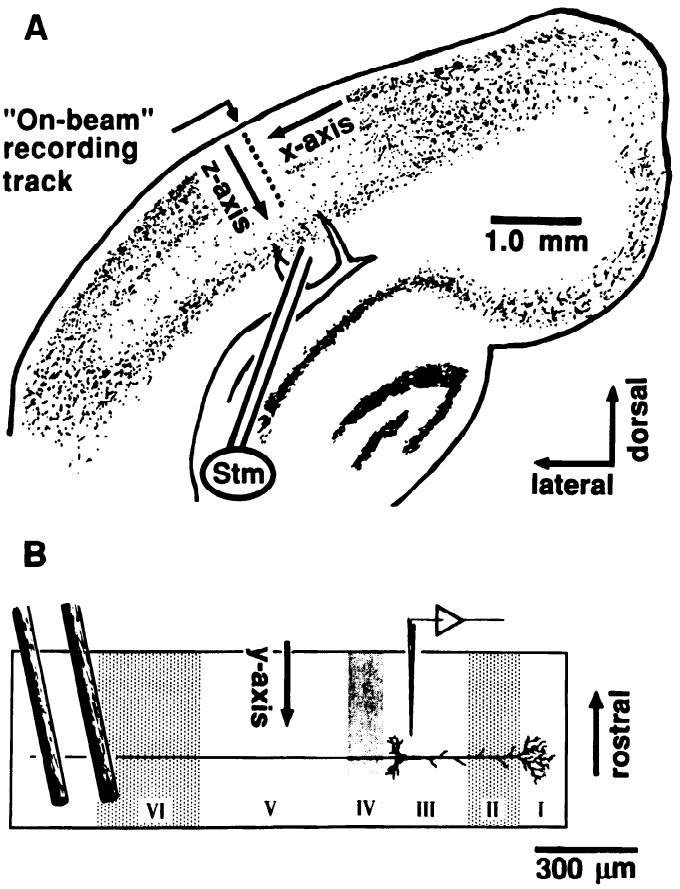


FIG. 1. The rat area 17 slice preparation. *A*: a typical slice, viewed from directly above the slice chamber. After recording, the slice was fixed, stained with cresyl violet, and its cytoarchitectural regions were traced. Area 17 is coextensive with the region where layer V is shaded more lightly. The stimulating electrode (Stm) was placed between 2 slits that transected the white matter underlying area 17. *B*: a cross-sectional diagram of a slice, viewed in the plane containing both the *z*- and *y*-axes. The stimulus electrodes (*left*), the cortical layers, the length and thickness along the *z*- and *y*-axes, and a layer III pyramidal cell are all shown to scale. The silhouette of the layer III pyramid is based on published Golgi data (Feldman 1984). Although the efferent axon is drawn exactly parallel to the plane of slicing, there may have been some rostral-to-caudal displacement of these axons as one moves toward the pia from the white matter (cf. Fig. 11).

colleagues (1984) examined transynaptically transported tracer after eye injections and concluded that conventional cytoarchitectural features correlate well with the extent of this region. As in other mammals, area 17 is characterized by dense packing of small cells in layer IV. In rat area 17, it may also be distinguished by the hypocellularity and breadth of its layer V. During cutting and in the slice chamber, the position in cortex was unambiguous because of contours in the shape of the subjacent hippocampus and the cortical white matter tracts. Recordings were made with slices taken in the coronal plane between 2.7 and 3.4 mm anterior to the interaural line (Paxinos and Watson 1986, Plates 41 to 44), distinguished by the presence of the granular layer of the dentate gyrus but absence of the corpus callosum. The location of recordings was confirmed by preparing Nissl-stained sections from slices (Fig. 1*A*).

### *Correlation of recording sites with cortical layers*

A central goal of this study was to relate physiological activity to identified cortical laminae. The recording electrode was therefore mounted on a micropositioner that allowed calibrated movements in the three orthogonal dimensions ($x$, $y$, and $z$, as defined above), and each recording position was precisely defined by the use of the pial surface and the $z$-axis, which intersected the site of stimulation as references. These positions were later compared with Nissl sections prepared from the same slices. The white matter lay 1,350–1,400 μm from the pial surface in both living slices and the Nissl sections; shrinkage of slices during fixation was therefore insignificant. In our material, as in published data (Parnavelas et al. 1977; Peters 1984; Peters and Kara 1985; Yamamoto et al. 1989), the border between layers I and II (at 125 μm depth), and that between layer VI and the white matter (at 1,350- to 1,400 μm depth) were completely unambiguous. The demarcation between layers IV and V (~650 μm depth) was also quite distinct; the border between III and IV was slightly less so, but there was a decrease in cell packing around 550 μm depth consistent with tracer transport data indicating that layer IV is only ~100 μm thick in the rat (Zilles et al. 1984). As is common practice, we refer to the cortex superficial to layer IV as "supragranular," and to layer II and III collectively as "layer II/III" because their boundary is indistinct. However, we refer to the region of layer II/III bordering layer I as "layer II," and the region bordering layer IV as "layer III."

### *Stimulation and recording*

Slices were stimulated with tungsten wires 50 μm in diameter and 150–200 μm apart lodged in the white matter as depicted in Fig. 1. We stimulated with square pulses (12–20 V for 50–75 μs) every 4 s. Currents up to 5 mA were needed to produce these voltages, presumably because the slices were submerged in 2–3 mm of medium. We expect that only a fraction of this current actually passed through the slice (see DISCUSSION, concerning the conductivity of the slice medium). Between stimulations, 0.2–0.4 V (0.2–0.5 μA) of opposite polarity was applied for 3 s to counteract polarization of the electrodes. In experiments in which the horizontal spread of excitation was studied, we sectioned the white matter with iridectomy scissors 0.5 mm medial and lateral to the site of stimulation (Fig. 1*A*). These radially oriented transections extended upward through most or all of layer VI. In most experiments, the column of cortex stimulated (3.5–4.0 mm lateral to the midline) was near the middle of area 17, with respect to its mediolateral extent.

Field potentials were recorded with broken-tipped glass micropipettes filled with 2 M NaCl (DC impedances of 5–25 MΩ) and advanced into the slice along the $y$-axis, from above. Except when otherwise indicated, data were recorded near midway between the rostral and caudal cut faces (100–300 μm into the slice with respect to the $y$-axis). The point of contact with the upward cut face was indicated by the tip movement artifact, rendered audible by passing the recorded signal through a voltage-controlled audiofrequency oscillator (Langdon and Jacobs 1980).

Superimposed on some field potentials, there occurred single-unit potentials, distinguishable as such because they were sensitive to minor alterations in the recording position and were all-or-none with respect to strength of stimulus. Normally, we avoided recording single units by *1*) advancing the electrode beyond an intended recording site then retracting back to it to do the recording, *2*) using broken-tipped electrodes, and *3*) averaging sets of 10–25 responses. In some experiments, however, we intentionally recorded unitary activity using unbroken glass micropipette electrodes (25–45 MΩ) and making fine advances along the $y$-axis. We used the same filter settings in either case (band pass from 0.1 Hz to 3 kHz). The data were then digitized at 5 or 10 kHz, either on-line or from recordings on video cassettes.

### *Current source-density (CSD) estimates*

Roughly speaking, negative field potentials are generated by (inward) current "sinks" and positive potentials by (outward)

current "sources," but depth potentials of field potentials offer only a poor approximation of the location of net inward and outward currents (Lorente de Nó 1947; Rall 1977). To better resolve the relationship of current flow to cortical laminae, we have calculated profiles of second derivatives with respect to the $z$-axis, using the sampling interval as our "differentiating grid." Provided that certain simplifying assumptions are valid, this amounts to a "one-dimensional CSD analysis" (Freeman et al. 1980; Haberly and Shepherd 1973; Nicholson and Freeman 1975). One such assumption is that net horizontal currents are negligible, which will be true only if voltage gradients are negligible along the $x$- and $y$-axes. Because stimulation was applied to a single location along the $x$-axis, we expected and observed response gradients along the $x$-axis. There also were gradients along the $y$-axis (see RESULTS). Nevertheless, we have derived and present estimates of CSDs. This is because most horizontal gradients were small relative to vertical gradients. Despite minor inaccuracies, CSD profiles may nevertheless help to characterize qualitative features of some response components. Moreover, we wished to allow direct comparison of our data with those of others who have estimated CSD profiles (Bode-Greuel et al. 1987; Perkins and Teyler 1988).

It is essential that responses be stationary through time when collecting data that will be used to estimate CSD profiles; small differences in the field potential produce relatively large current density estimates. Thirty to 40 min were required to record a depth profile. Except as noted, the response components that we present differed very little over such intervals, and we present only those features of CSD profiles that were observed consistently.

## RESULTS

The first half of our presentation of results will specifically concern on-beam responses, and the latter portion will describe activity horizontal to the stimulated beam. On-beam, normal responses were composed of one or more rapid negative deflections during the first 20 ms and slow components lasting roughly 50–100 ms (Fig. 2*A*). The rapid deflections appeared to be population spikes (see below) and will be referred to as such, or more simply as "spikes." In layer III, prominent spikes occurred in short bursts ("S1" and "S2" in Fig. 2*A*). Most preparations exhibited at least one fast potential in layer III that was ≥0.5 mV in amplitude, and we used the presence of this response component as a minimal criterion for regarding a preparation as viable and the stimulation level adequate. Layer III spikes became a major focus of our investigation and are dealt with in greater detail in a later section. There were also bursts of low-amplitude spikes in layer V. These were typically <0.15 mV in amplitude and were not systematically studied.

We believe that the response components that we designate as "field potentials" represent synchronized activity of *populations* of neurons because even our most focal field-potential components (the "S1" population spikes) exhibited nearly the same latency, shape, and amplitude for 200–500 μm along the $x$-axis and for 150–300 μm along the $y$-axis (see below). Moreover, amplitudes of these spikes were graded with respect to stimulus strength (Fig. 3), a feature that is completely uncharacteristic of single-unit spikes.

### *Slow waves "W1" and "W2"*

There were two conspicuous slow-wave components, "W1" and "W2," with maximum negativities in layers II and III, respectively (Fig. 2). In contrast to the population spikes (S1 and S2), these were accompanied by a relatively large positive potential in layer I. Component W1 was larger and of shorter duration than W2. It peaked 10–20 ms after stimulation, and it decayed during the following 50–100 ms. In depth profiles, it was negative in upper layer II, with the polarity reversing abruptly at ~125 μm subpial depth (the border between layers I and II). Often, there also occurred a smaller positive waveform in layer III of similar time course.

The time course of the initial rise of component W2 was ambiguous because of superimposition on component W1. Component W2 peaked at ~100 ms and decayed over

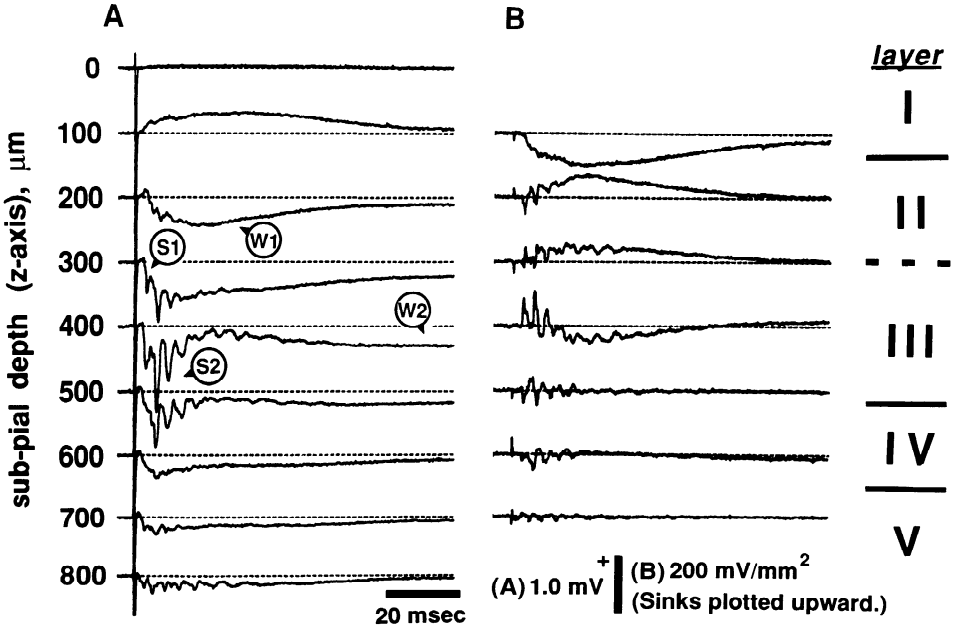


FIG. 2. Profiles of responses recorded along the $z$-axis directly radial to the site of stimulation (on beam). *A*: normal field potentials. *B*: estimates of the net densities of current sources and sinks, derived from the data in *A*. Fast components are labeled as S1 and S2, and slow components as W1 and W2 as described in the text.

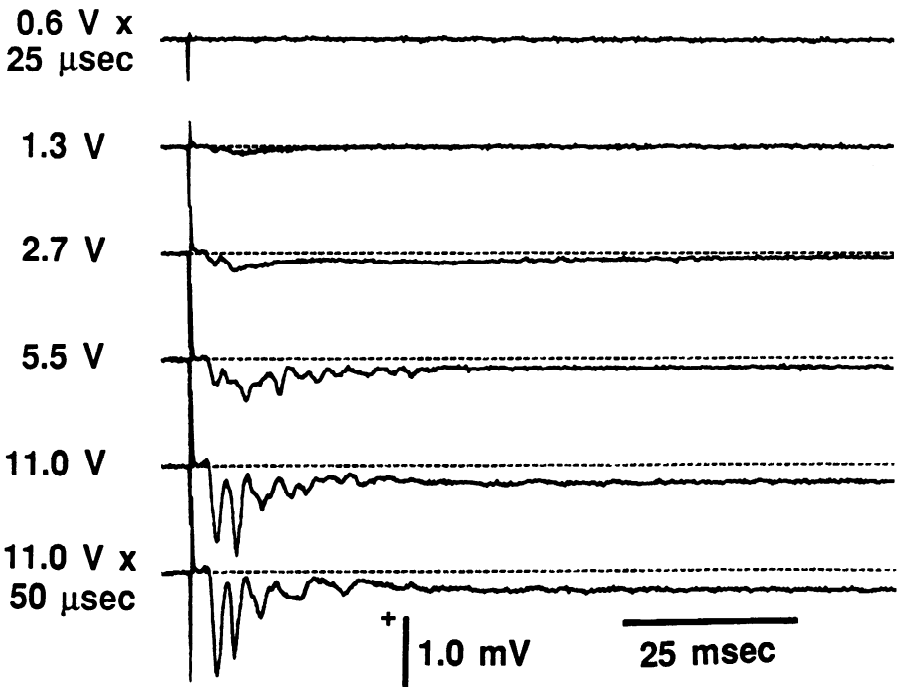


FIG. 3. Responses on beam in layer III as a function of stimulus strength.

several hundred milliseconds thereafter. Under normal conditions, its amplitude was quite low and its depth distribution diffuse. Its presence varied from one preparation to the next. We have devoted only minor attention toward it as a component of normal responses, but note that the application of $Mg^{2+}$-free medium enhances this component considerably (Langdon et al. 1988a; Langdon and Sur, unpublished observations).

Derivation of profiles of CSD estimates appeared to give an improved definition of component W1. The sink activity responsible for W1 was limited to layer II, just below the border with layer I (Fig. 2*B*). The field potential at this depth provided a reasonably good estimate of the time course of component W1 because the field potential associated with W2 reversed in polarity at this depth (and hence was null). The current that generated component W1 rose to a peak within 20 ms. Its decay to 37% (1/e) of peak amplitude typically required 20–30 ms. In CSD profiles, component W2 was present only as a very low-amplitude sink density in layer III, after decay of component W1.

*Component S1, the directly conducted spike*

It is generally believed that rapid, concerted release of neurotransmitter depends on the presence of extracellular $Ca^{2+}$ (Dingledine and Somjen 1981; Hackett 1976; Katz 1969; Krnjević 1974; Langdon et al. 1988b; Richards and Sercombe 1970). We therefore examined responses in slices maintained in $Ca^{2+}$-free medium to determine which response components did not depend on synaptic transmission. Slow waves W1 and W2 and all rapid deflections after 5 ms were eliminated by $Ca^{2+}$-free medium (Fig. 4). During the first 5 ms poststimulation, however, there occurred a large, rapid negative deflection that retained nearly the same amplitude and latency in $Ca^{2+}$-free medium as it had in normal medium (Figs. 4–6). We refer to this $Ca^{2+}$-independent spike as "component S1," to distinguish it from the "S2" spikes that follow it. (We will use the terms "component S1" and "direct spike" synonymously.) In layer III, component S1 peaked 2–5 ms after stimulation with amplitudes up to (−)2.5 mV. With increasing depth, the latency of component S1 grew shorter. From ~150–300 μm depth, component S1 began with a small positive deflection (Fig. 5). From the pial surface to 150 μm, the positive deflection was larger and longer, and no negative deflection followed. In normal medium, component S1 was followed by one or more similar S2 spikes (see below), and both the S1 and S2 spikes rode on a negative envelope that decayed quickly as slow wave W1 began. In $Ca^{2+}$-free medium, there was no appreciable slow wave associated with S1.

The laminar distribution of component S1 approximated the distribution of the somata of neurons that send slowly conducting axons to the white matter (Swadlow and Weyand 1981; see also Gilbert 1983; Gilbert and Wiesel 1981; Jones 1984, 1988). It was absent in layer I, a target of ascending afferents. It was the largest in layer III (Figs. 4 and 5) and was smaller in layer IV than in either III or V. As we discuss in greater detail later, the data were most consistent with the conclusion that component S1 represents synchronous firing by cortical pyramidal cell somata activated antidromically via their efferent axons. To test this hypothesis, we observed the effect of muscimol on component S1 in $Ca^{2+}$-free medium. Assuming that there are γ-aminobutyric acid (GABA)-gated $Cl^-$ channels in the plasmalemma of the cell somata and proximally in the dendrites, then the presence of a GABAergic agonist in the bath should decrease the number of somata antidromically invaded or otherwise diminish the amplitude of the population spike by increased current shunting. Consistent with this, we observed a 30–40% attenuation of the direct spike when 10 μM muscimol was included in the $Ca^{2+}$-free bathing medium (not shown).

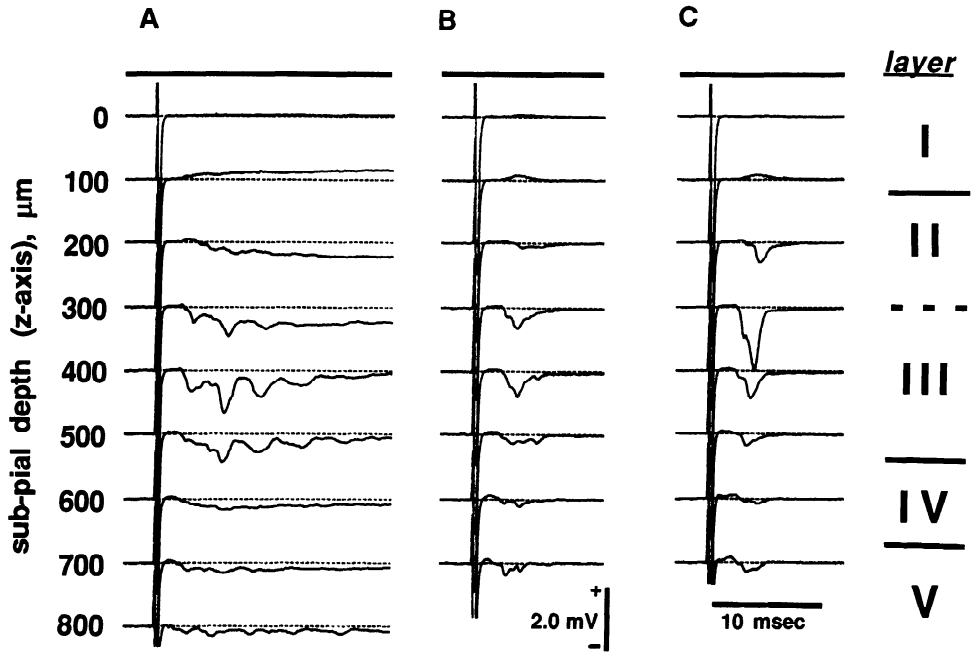


FIG. 4. Depth profiles of field potentials, comparing responses (*A*) with $Ca^{2+}$ in the medium and (*B* and *C*) without $Ca^{2+}$. *C* was recorded directly on-beam; *A* and *B* were recorded along the *z*-axis 300 μm medial to *C*.

*Component S2: repetitive firing in layer III*

When slices were bathed in normal medium, component S1 was usually followed by one or more fast waves in layer III (S2 in Fig. 2*A*). These individual waves had much in common with each other and with component S1. Individual S1 and S2 spikes exhibited the same shape and time course. There was a close correlation of their amplitudes, compared with respect to depth (Figs. 2 and 5). There was no apparent shift in the laminar distribution of the individual spikes as the bursts progressed.

We have considered that these repetitive spikes might be a form of epileptiform activity, and therefore compare our data with field potentials recorded from slices in which epileptiform activity was induced by applying the GABA antagonist, bicuculline (Chagnac-Amatai and Connors 1989a; Chervin et al. 1988; Connors 1984). There are a number of differences. Amplitudes of S1 and S2 spikes increase in a graded fashion as the strength of stimulation increases (Fig. 3), whereas response latencies remain unchanged. Recorded on-beam, the S1 spike consistently occurs between 2.5- and 4.5 ms latency (Fig. 6), and the first S2 spike follows 2.5–4 ms later (Fig. 7). In contrast, the latency, and not the amplitude of evoked epileptiform activity, varies with the strength of stimulation. The latency of epileptiform responses may be as long at 100 ms, and varies with each individual trial. We observed long-latency burst responses with low-strength stimulations in one preparation; otherwise, stimulus strength did not much affect latency.

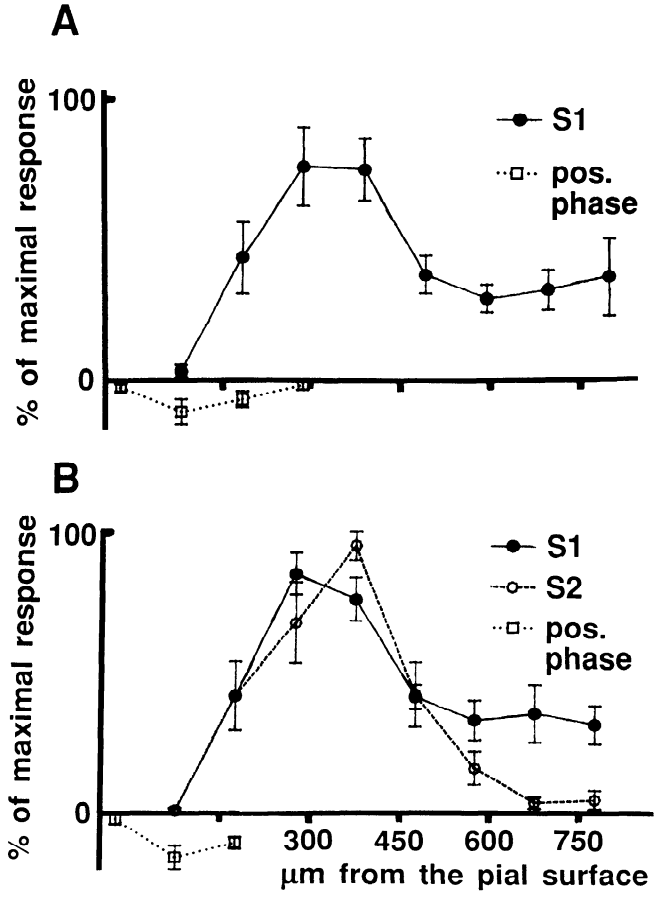


FIG. 5. Mean amplitudes of early population spikes as a function of depth (along the *z*-axis); data from 7 on-beam depth profiles, each from a different preparation. Before averaging, each component in each profile was normalized to its maximal amplitude. Each error bar represents 1 SE. *A*: mean amplitudes of S1 spikes in $Ca^{2+}$-free medium. The mean maximum amplitude was −1.65 mV (range, −0.72 to −2.86; 1 SD, 0.77). *B*: mean amplitudes of components S1 and S2 in depth profiles in normal medium. At depths of ≤200 μm, no unambiguous distinction could be drawn between components S1, S2, and W1. The mean response amplitude indicated for depth ≤200 μm is simply that of the negative deflection that occurred there 5–10 ms after stimulation. At depths of ≤200 μm, the negative deflections were preceded by a small positive deflection. Mean amplitudes of these (relative to the amplitude of maximal negative deflections) are indicated by the squares connected by dotted lines. For the profiles in *B*, the mean maximal S1 amplitude was −1.14 mV (range, −0.66 to −1.73; 1 SD, 0.37). For S2 spikes, the mean maximum was −0.67 mV (range, −0.16 to −1.86; 1 SD, 0.57).

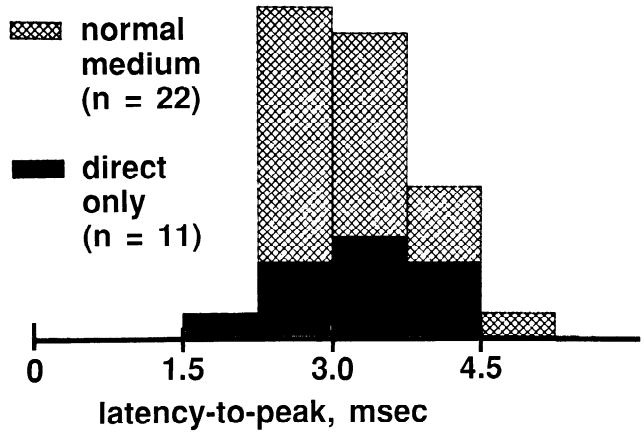


FIG. 6. The distribution of latencies of component S1 when recorded near the beam center in layer III. Each sample was from a different slice preparation. The amplitudes of spikes recorded in normal medium ranged from 0.6 to 2.2 mV with a mean of 1.3 mV (1 SD, 0.54). The group designated "direct only" included 9 samples from slices in $Ca^{2+}$-free medium, and 2 in normal medium containing 10 $\mu$M CNQX (cf. Fig. 10). The mean amplitude in the direct only group was 1.7 mV (range, 1.0–2.9; 1 SD, 0.68).

Repeating population spikes (indicative of phase-locked firing) are not a prominent feature of "paroxysmal field potentials" recorded during epileptiform episodes, whereas our responses consist primarily of large spikes followed by low-amplitude slow waves. Averaged responses closely resemble single traces, indicating that the individual spikes in these bursts are tightly phase locked not only to the stimulation but also to each other.[1] Amplitude decays rapidly after the first or second spike in a burst, so that these trains of repeating spikes fade into the background noise within 15–20 ms. Only minor potentials (<0.4 mV) persist beyond ~40 ms. In contrast, epileptiform events exhibit prominent slow field-potential waveforms that continue for hundreds of milliseconds.

Component S2 occurs only in layer III. In contrast, epileptiform events are characterized by large field potentials spanning the entire thickness of the cortex. The distinction is perhaps best appreciated by considering layer IV. In our response profiles, activity in layer IV was minimal (Fig. 2, 600 $\mu$m depth). In contrast, during the epileptiform paroxysm, layer IV activity is quite prominent (Connors 1984, Fig. 1*c*).

In summary, component S2 is a phenomenon distinct from (but perhaps related to) epileptiform activity as the latter has been described in slices of neocortex treated with bicuculline. We do not use the term "component S2" to refer to any loosely defined burst of fast-wave activity. Rather, this component is a highly stereotypic pattern of evoked activity limited to layer III in our slices. We regard components S1 and S2 collectively as due to synchronized firing of what is most likely a single neuronal population in layer III.

[1] In studies of cellular mechanisms of epileptiform activity, reference is often made to "synchronous" firing or bursting (e.g., Alger et al. 1984; Connors 1984). Usually, no distinction is specified between synchronized bursting and synchronization of individual firings within bursts. We wish to make this distinction, and therefore refer to synchronization of individual firings as "phase-locked" firing or bursting.

As a means of examining the cellular basis of components S1 and S2, we recorded single-unit activity between depths of 300 and 400 $\mu$m ($z$-axis). More specifically, we recorded extracellular spike activity, considering this approach less likely than intracellular impalements to alter

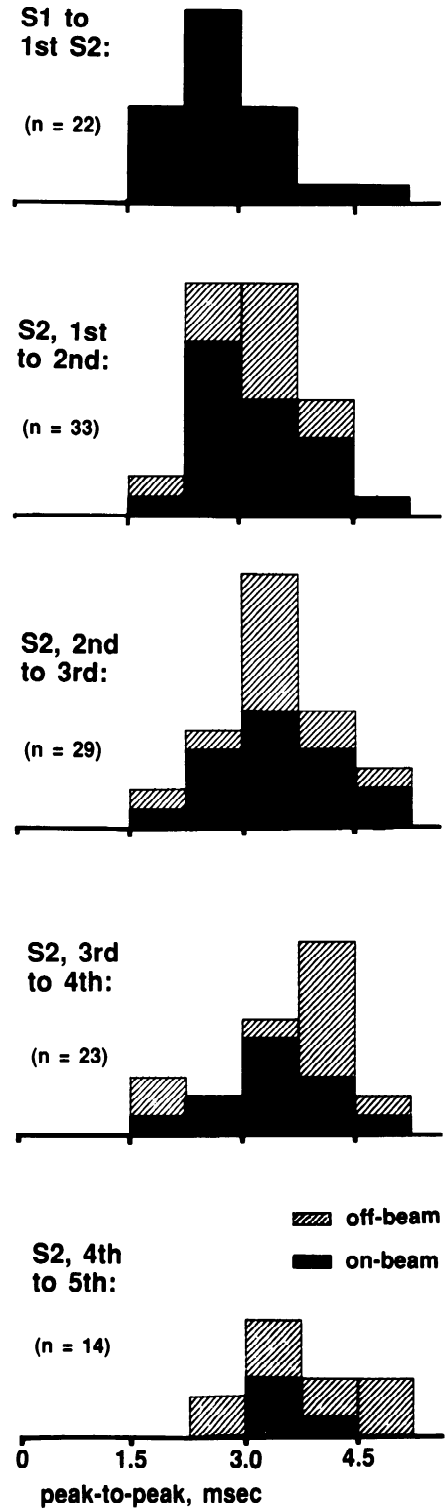


FIG. 7. Histograms illustrating the distribution of successive interspike intervals after the S1 spike. The data are from 25 slice preparations, with no more than 1 on-beam value or 2 off-beam values derived from each; the latter were recorded at least 600 $\mu$m apart. The sample size decreases because not every burst included a discernable 3rd, 4th, or 5th spike.

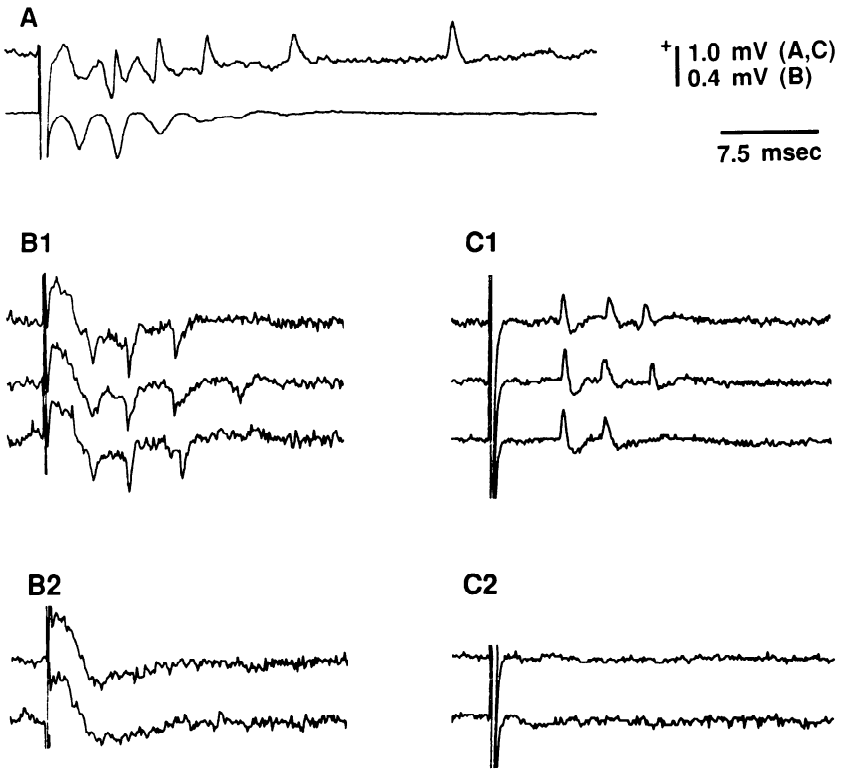


FIG. 8. Evoked single-unit activity in layer III. All responses were recorded within 400 $\mu$m of the beam center with the use of glass micropipette electrodes. *A*: 2 recordings from the same location and with the same electrode, but made 40 min apart. In the *top*, unitary extracellular spikes (the upward deflections) and field potentials are superimposed. After contact with this unit was lost, there remained a field potential composed of S1 and S2 spikes (*bottom*, an average of 25 trials). *B*: recordings of a different cell, comparing responses to stimulus of 17 V (*B1*) and 12 V (*B2*). *C*: a 3rd cell, recorded in normal medium (*C1*) and in $Ca^{2+}$-free medium (*C2*) (stimulus, 16 V for both).

neuronal firing patterns. Under conditions that generated field-potential components S1 and S2, we readily encountered units that fired bursts of 2–6 spikes (Fig. 8). We regarded these as individual units (and not field potentials) principally because they occurred in an all-or-none fashion (Fig. 8, *B* and *C*). These units showed no evidence of injury-induced discharge; fine movements of the electrode did not elicit firing, and firing occurred only after stimulation. We recorded 15 such units in 8 slice preparations for intervals of $\geq$10 min. In general, these spikes were composed of positive, then negative phases (Fig. 8*C*), but we observed a complete range from spikes that were nearly positive only (Fig. 8*A*) to purely negative (Fig. 8*B*). Presumably, any individual neuron could generate a unitary potential of any of these shapes, depending on whether membrane along the soma, dendrites, or axon was apposed to the recording electrode. Therefore we did not restrict our attention to unitary potentials with the same shape as the field-potential spikes.

To determine whether or not unitary and field-potential spikes shared a common latency, an unambiguous distinction between the two phenomena was required. When purely negative single-unit spikes were superimposed on field-potential spikes, the discrimination between the former and the latter was sometimes ambiguous (e.g., the first spike in the second trace in Fig. 8*B1*). Analyses of spike latencies were thus restricted to recordings of units with a positive component. In some recordings, such unitary spikes were superimposed on field-potential spikes (Fig. 8*A*), so that the correlation of latencies was self evident. We also recorded unitary spikes in locations where field-potential spikes were small or absent (Fig. 8, *B* and *C*), such as near the upward face of slices. In these latter cases, latency histograms revealed that unitary spikes coincided closely with typical S2 latencies (i.e., ~6, 10, and 13 ms; Fig. 9). We also observed some units that fired only once, and not all repeating spikes coincided with typical S1 and S2 latencies. However, it was clear from our recordings that units that fired in synchrony with S1 and S2 spikes were quite common in layer III.

We considered that the field-potential components S1 and S2 may result from the synchronized but, otherwise, independent firing of intrinsically bursting neurons (Chagnac-Amitai and Connors 1989b; McCormick et al. 1985), with the firing coherence simply the result of synchronous initiation of bursting. Although the bursts required me-

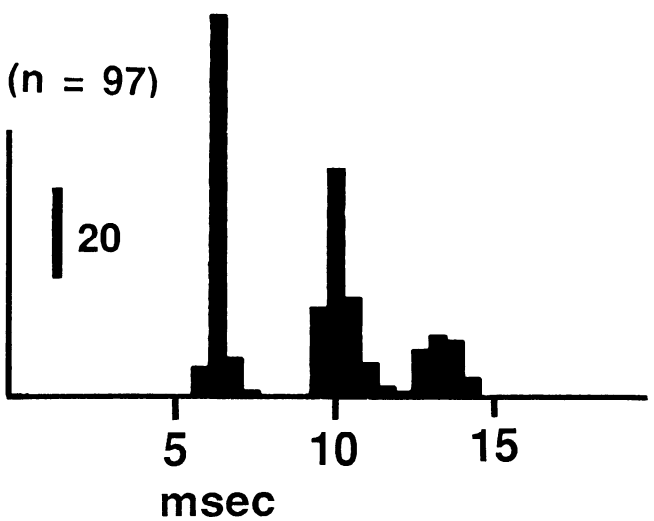


FIG. 9. A histogram of the latencies of spikes evoked in 97 trials performed on the cell in Fig. 8*C*. Any deflection of −0.45 mV or more over an interval of 0.5 ms was counted as a spike. The mean response was 2.42 spikes/stimulus.

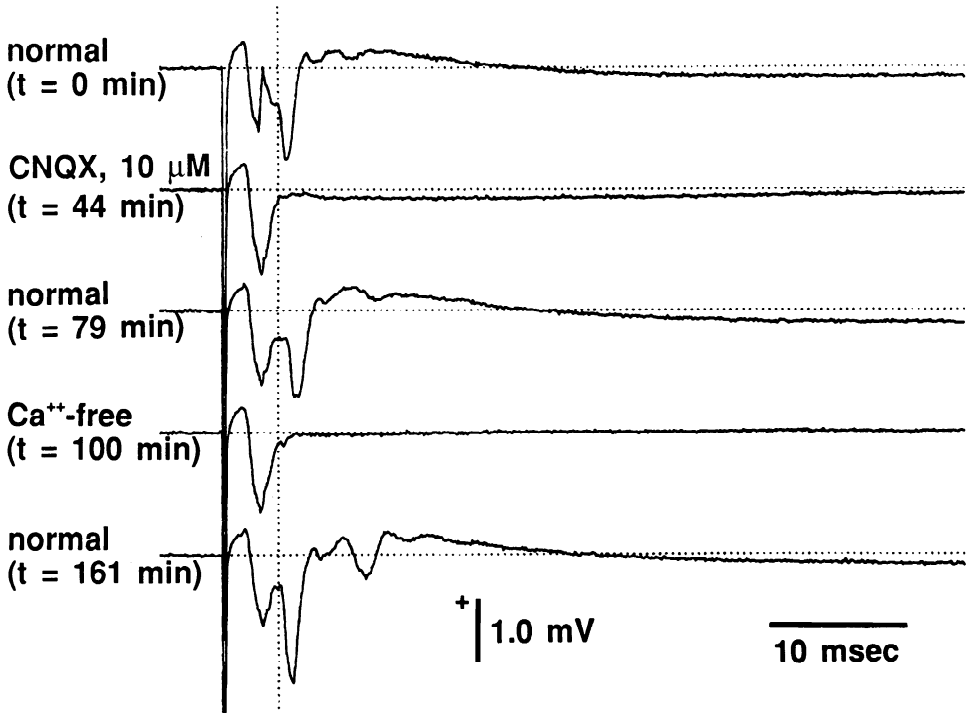


FIG. 10. Block of $Ca^{2+}$-dependent spikes and slow waves by 10 $\mu$M CNQX, an antagonist of excitatory amino acid receptors of the "non-NMDA" subtype. Responses were recorded on beam in layer III.

dium containing $Ca^{2+}$, it remained unclear whether this was due to a need for $Ca^{2+}$-mediated release of neurotransmitter, or dependence on a somatic (or dendritic) $Ca^{2+}$ spike. Application of the glutamate receptor antagonists kynurenic acid or 6-cyano-7-nitroquinoxaline-2,3-dione (CNQX) led to failure of spikes occurring after 5 ms latency; i.e., the same spikes that depended on extracellular $Ca^{2+}$ (Fig. 10) (also, Langdon et al. 1988a, and unpublished observations). It was therefore concluded that all spikes after 5 ms are synaptically enabled or driven.

CSD profiles suggested that the current generated by synchronous spike activity in layer III flowed inward at one sampling depth only (Fig. 2*B*). (In contrast, the spike field potential was distributed across 3 consecutive sampling depths spanning 300 $\mu$m.) However, these CSD estimates represent *net* current densities; zones where inward current was present at a relatively low density may appear inactive because of superimposition of outward current flowing passively from adjacent regions of high sink activity. Hence these CSD profiles may underestimate the true vertical extent of activated neuronal membrane.

In the METHODS section, we reviewed some assumptions on which one-dimension CSD estimation is based. These assumptions were more valid for some response components than for others. All fast and slow events described to this point were temporally stationary. Concerning the accuracy of CSD estimates based solely on profiles along the *z*-axis, the slow components varied only gradually with horizontal displacement of the recording site (see below). However, some of the population spikes were very sensitive to horizontal displacement.

*Horizontal distributions of responses*

In contrast to their relationship in depth profiles, the distributions of direct (S1) and synaptically driven (S2) spikes often differed appreciably in horizontal profiles; i.e., those recorded by displacing the recording electrode along the *y*- or the *x*-axes while remaining in layer III. With regards to the *y*-axis, the direct spike tended to be larger nearer to the caudal cut face, whereas S2 spikes tended to be largest close to the midplane between the cut faces (Fig. 11). However, our most detailed data concerning horizontal distributions relied on displacements of the recording site along the *x*-axis. As with on-beam responses, we determined which components depended merely on axonal conduction by collecting profiles of direct spikes in either $Ca^{2+}$-free or CNQX-containing medium and compared

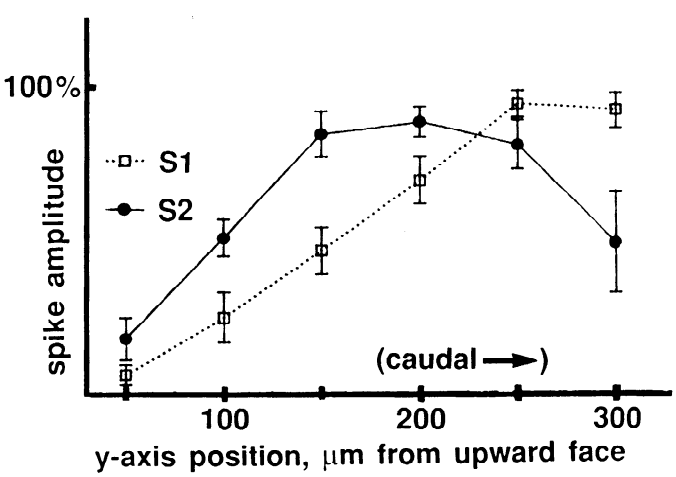


FIG. 11. Comparison of the amplitudes of S1 and S2 spikes with respect to displacement along the *y*-axis, averages from 7 preparations in which the caudal cut face was downward. Before averaging, each profile was normalized with respect to its own maximum. The mean maximum amplitude of S1 spikes was −0.99 mV (range, −0.30 to −1.43; 1 SD, 0.50) and for S2 spikes was −0.65 mV (range, −0.16 to −0.96; 1 SD, 0.34). All profiles were sampled in layer III within 400 $\mu$m of the beam center (*x*-axis distance).

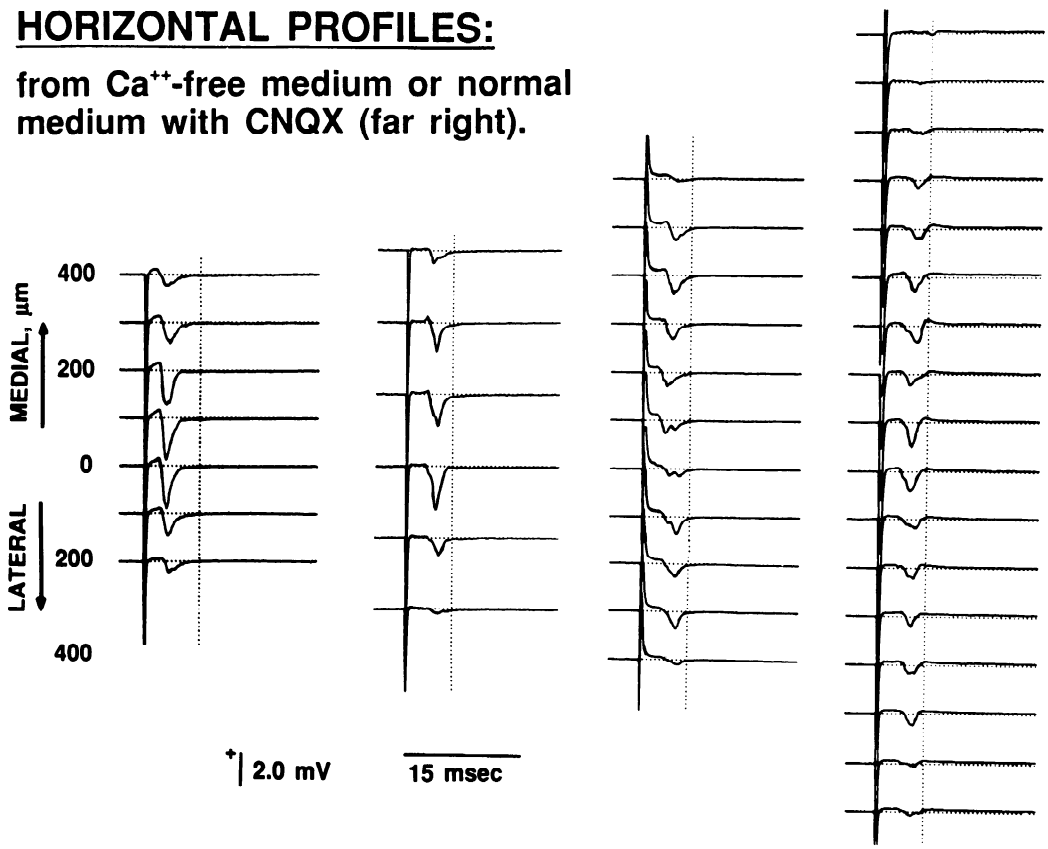


FIG. 12. Horizontal distributions of direct spikes isolated by medium containing CNQX or no $Ca^{2+}$. Each profile is from a different slice. The vertical dotted lines are placed 6 ms after stimulation.

these with profiles from normal medium. Horizontal distributions of direct spikes varied from highly localized and unimodal (Figs. 12 and 13*A*) to relatively disperse with two local maxima (Fig. 12, profile at *far right*). However, large direct spikes did not occur beyond 400 μm from the beam center nor after 6 ms latency. The relationship between latency and horizontal displacement suggested that either off-beam or on-beam, direct spikes were conveyed by axons that conducted at the same velocity; the increase in latency of direct spikes was roughly proportional to the length of the diagonal from the stimulation site to the recording site, with conduction at ~0.3 m/s.

In normal medium, as in $Ca^{2+}$-free or CNQX-containing medium, spikes with latencies <5–6 ms and amplitudes >0.5 mV did not occur farther than 400 μm from the beam center (Figs. 13*B* and 14*A*). In contrast, synaptically driven responses (that is, of latencies >6 ms) occurred over a broad and variable distribution, with field-potential spikes

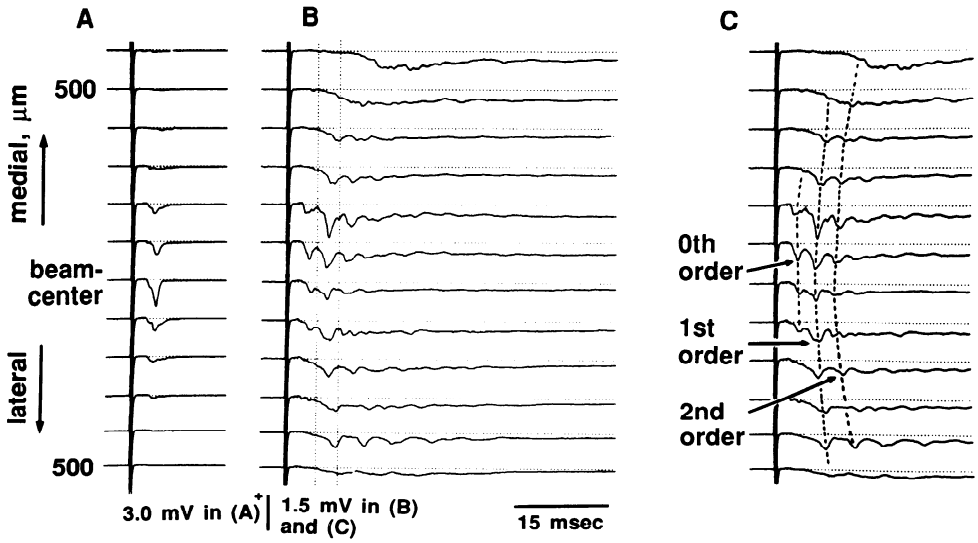


FIG. 13. A typical horizontal (*x*-axis) profile sampled at 100-μm intervals in layer III. *A*: in $Ca^{2+}$-free medium. *B*: recordings from the same slice and *x*-axis positions in normal medium. The *y*-axis positions for the recordings were chosen to be optimal for direct spikes in *A* and for S2 spikes in *B* (cf. Fig. 11). Therefore the direct spikes are larger in *A* than in *B*. *C*: an interpretation of the synaptic order underlying the population spikes in *B*.

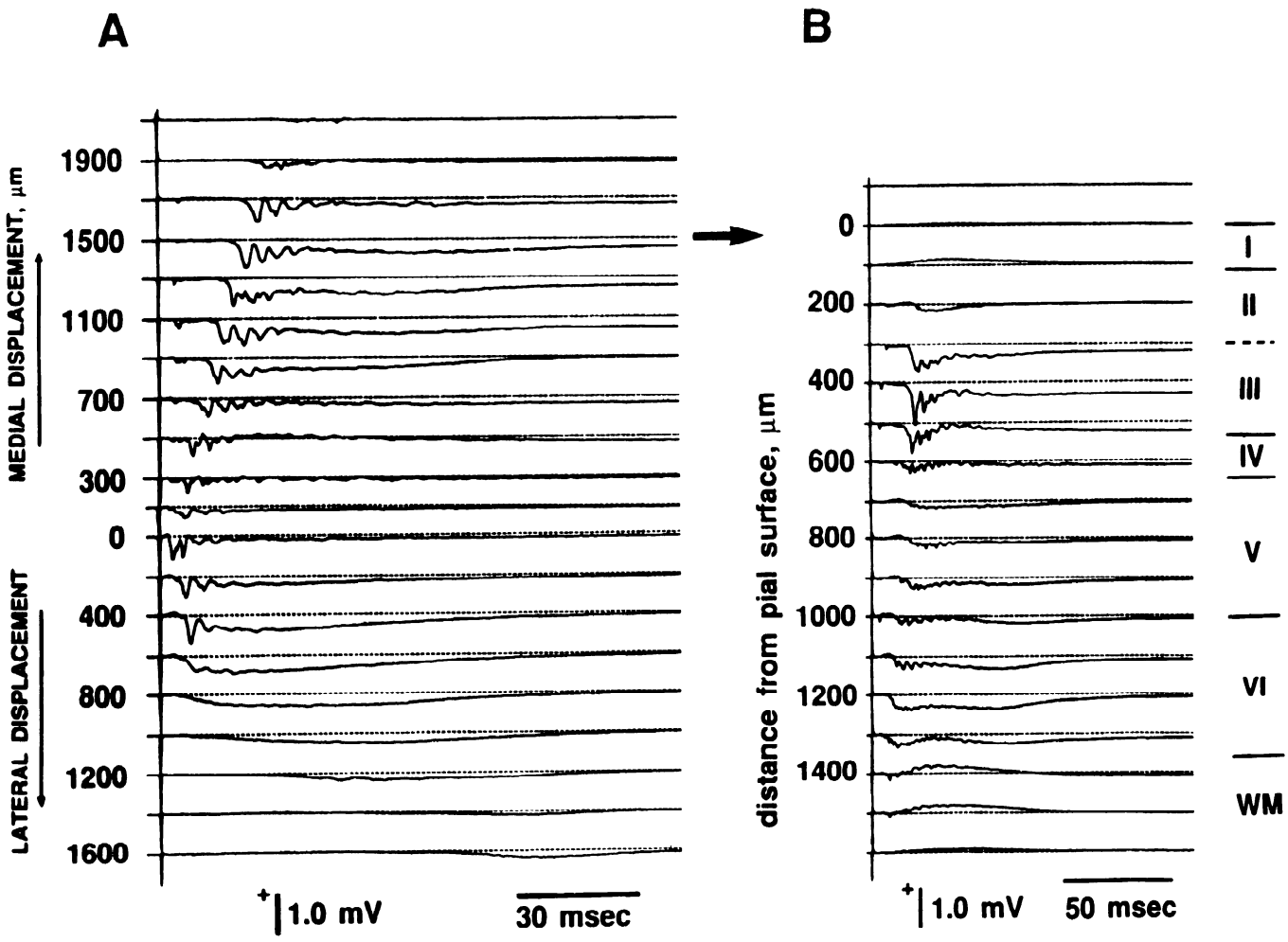


FIG. 14. An example of far-ranging horizontal spread of activity. *A*: horizontal profile recorded in layer III. *B*: a depth profile recorded 1.5 mm medial to the beam center.

as far as 1.8 mm from the beam center. Figures 13*B* and 14*A* present, respectively, examples of modest and extreme spread of activity. Regardless of the extent of horizontal spread, off-beam depth profiles bore considerable resemblance to those recorded on beam (cf. Figs. 14*B* and 2*A*). As with on-beam depth profiles, repeating population spikes in layer III comprised the largest response component, and these bursts of large spikes occurred only in layer III. They exhibited the same frequency, duration, and depth distribution off-beam as they did on-beam. Off-beam responses were phase locked to stimulation and of constant latency, even when this latency was as long as 25 ms.

We propose that the S2 spikes are driven to fire in phase by excitatory horizontal projections (collaterals) of layer III cells, with synchronous firing of these latter initiated by antidromic activation. To characterize the relationship between horizontal distance and the strength of such projections, we analyzed profiles with respect to latencies and amplitudes. The latency of layer III spikes increased by 10–15 ms for each millimeter of horizontal displacement (Figs. 13*B* and 14*A*), a rate of spread roughly three times slower than conduction of impulses from the white matter to layer III. The earliest S2 spikes (labeled "1st order" in Fig. 13*C*) occurred within a few hundred microns of the zone of direct activation (labeled "0th order" in Fig. 13*C*). Over this range, the first S2 spikes in adjacent regions (sampling every 100 or 200 μm) occurred within 0.5 ms of each other. Beyond this 1st order range, spikes were either absent (e.g., Fig. 13) or occurred after an additional 3–4 ms of latency (e.g., Fig. 14*A*, the response 700 μm medial to the beam center begins 3.2 ms later than at 500 μm medial). One interpretation would be that the short-latency S2 spikes occur over the range in which horizontal projections are especially dense. To estimate this range, we measured the amplitudes of S1 and short-latency S2 spikes in six horizontal profiles, normalized these with respect to each distribution's maxima, and then calculated profiles of the average amplitudes (Fig. 15). The resulting pattern implied that horizontal connections in layer III are particularly strong over distances of ≤400 μm.

In the example of extreme horizontal spread (Fig. 14), repeating layer III spikes occurred for only 400 μm lateral to the beam, but for 1700 μm medially. (Stimulation was centered midway between the medial and lateral boundaries of area 17.) It was typical for far-ranging horizontal spread to occur in the medial direction only. Beyond the medial and lateral ends of the zone in which layer III population bursts were present, there was usually a region exhibiting a slowly rising and falling negative wave in layer III.

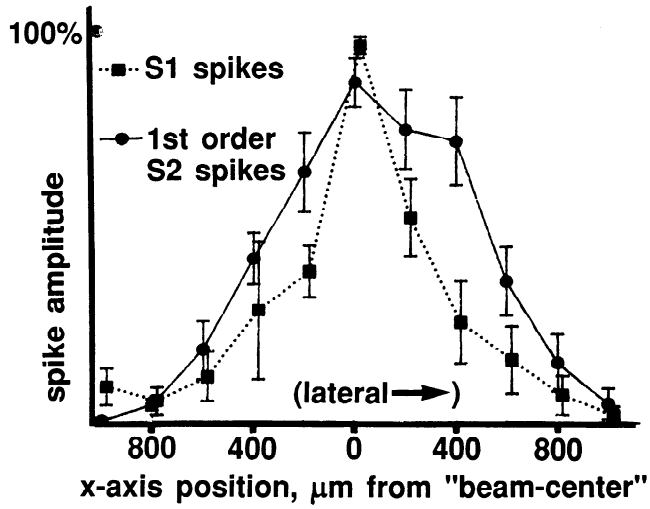


FIG. 15. Comparison of the relationships of amplitudes of S1 and "first-order" S2 spikes to position along the *x*-axis; data averaged from 6 different preparations. These average profiles were derived as described in the text. On beam, all S1 spikes occurred between 2.5- and 5-ms latency, and S2 spikes between 5 and 9 ms. Means ± 1 SE are indicated. The mean peak S1 amplitude was −0.67 mV (range, −0.29 to −1.47; 1 SD, 0.42), and the mean peak S2 amplitude was −1.38 mV (range, −0.68 to −2.00; 1 SD, 0.43). All recordings were made near the slice midplane, which is not necessarily optimal for direct spikes; hence, the mean S1 amplitudes are smaller.

When recording laminar depth profiles far off-beam, it was practical, unlike with on-beam profiles, to extend recordings all the way to the white matter because the track of recording sites did not approach the stimulation site. We thereby obtained recordings of potentials in layers V and VI that would otherwise have been obscured by the stimulus artifact. These revealed an abrupt negative deflection in layer VI and lower layer V followed by some low-amplitude, repeating fast waves and a slow negativity lasting ~100 ms (Fig. 14*B*). This activity in layers V and VI preceded the spike bursts in overlying layer III by 9 ms. As with on-beam responses, layer IV was nearly devoid of activity. In layer III, the spike burst was followed by a long, slow negativity, as it was on-beam.

*Response variability*

Besides (or related to) the variability in the extent of horizontal spread of responses, the amount of synaptically driven activity directly on beam varied from one preparation and stimulus placement to the next; the reasons remain unknown. Postsynaptic activity did not depend merely on good slice variability because some preparations exhibited S1 spikes 2 mV or more in amplitude, but little else (not shown). This variability was seen between preparations, but with any particular preparation and stimulation site the amount of postsynaptic activity remained relatively constant over a period of hours.

In a few preparations we observed slow negative waves that began 30–100 ms after stimulation. These rose for 10–20 ms to reach peak amplitudes of ~1 mV and then fell over several additional tens of milliseconds (not shown). In time course, these responses thus resembled late depolarizations recorded intracellularly by Artola and Singer (1987, their Fig. 1, *a* and *b*), either in normal medium or, more often, in bicuculline-treated slices. Like their "bursting cell" responses, our slow waves were usually eliminated by interstimulus intervals of <10 s. Similar intracellular data have come from Sutor and Hablitz (1989; their "late EPSP"). Unlike our four main response components, these slow waves varied considerably from trial to trial. We did not systematically study these responses.

## DISCUSSION

In slices of rat visual neocortex in vitro, we have examined profiles of field potentials sampled radially within cortical columns, and horizontally within layer III, activated in either case by electrical stimulation applied near the border between the underlying white matter and layer VI. A goal of this study was to improve definition of normal field potentials in physiological slices of visual neocortex so that more meaningful comparisons may be made between data from different experiments and experimenters when field potentials are used to assess neocortical pharmacology and plasticity of synaptic connections (Hamasaki et al. 1987; Kimura et al. 1989; Komatsu et al. 1988; Langdon et al. 1988a, 1989; Lee 1982; Perkins and Teyler 1988; Yamamoto et al. 1989). Beyond this, we wished to extend our present understanding of the physiology and organization of neocortical circuitry. Toward these ends, we propose a decomposition of these responses into four component population events. This discussion will concern the neurons, connections, and physiological activities likely to underlie these response components. More specifically, we will discuss *1*) our field-potential data in comparison to those from previous studies, *2*) the neocortical cell types that we regard as most likely to be responsible for these component population events, and *3*) the implications of our findings with respect to normal and pathological activities of the neocortex.

*Component W1: a neocortical field EPSP?*

The analysis of field-potential data has been rigorously discussed in the literature (Freeman et al. 1980; Haberly and Shepherd 1973; Llinás and Nicholson 1974; Lorente de Nó 1947; Mitzdorf 1985; Nicholson and Freeman 1975; Nicholson and Llinás 1971; Rall 1977; Rall and Shepherd 1968). The generation of a field potential requires three conditions: *1*) synchronous activation of a neuronal population; *2*) flow of current in a population of loops that include an adequate extracellular leg; and *3*) some element of parallelism in the geometry of this population, so that the elemental currents do not cancel each other. Because of these constraints, field potentials are most often observed in neuronal fields in which apical dendrites are oriented in parallel. In the hippocampus, the field potential generated by the flow of neurotransmitter-gated current in such apical dendrites is referred to as a "field excitatory postsynaptic potential (EPSP)" (Andersen et al. 1978, 1980). In depth profiles it consists of a rather slowly decaying dipole. There are many other systems in which an analogous field potential occurs (cf. Haberly and Shepherd 1973; Langdon et al. 1988b; Llinás and Nicholson 1974; Rall and Shepherd 1968), although the term "field EPSP" is used less often regarding these systems.

Apical dendrites in the neocortex are laid out in parallel, but there is no layer of cortex ideally suited for generation of a *discrete* field EPSP because there is no layer that receives an isolated afferent tract. We do observe, however, two relatively slow field-potential dipoles (and source-sink pairs) oriented parallel to the supragranular apical dendrites. We have named these components W1 and W2. Under normal conditions, the second of these is much smaller and more variable than the first. We confine our discussion to W1, but analogous considerations apply to W2.

The sharp reversal in the field potential at the border between layers I and II must result from a substantial flow of current toward layer I within the dendrites crossing that border. This implies excitatory activity that occurs specifically in layer II and not in layer I. Component W1 depends on excitatory neurotransmission, presumably through synapses concentrated in layer II where net sinks are revealed in CSD profiles. Hippocampal field EPSPs are most typically evoked by stimulating afferents presynaptic to the more distal regions of apical dendritic arbors. However, when stimulation is delivered only to those afferents that contact the dendrites proximally, profiles of the evoked field potential indicate that the intradendritic current flows from proximal to distal (Andersen et al. 1980). We propose that this same current orientation generates component W1.

The presynaptic element remains unknown, however, and it is questionable whether a single synchronous activation of excitatory inputs could lead to a current with a time course as prolonged as that of component W1. The passive cable properties of dendritic arbors should constrain the decay of a truly subthreshold field EPSP to continue for a certain minimal duration, regardless of the brevity of the initial ligand-gated synaptic current (Langdon et al. 1988b; Rall 1969, 1977). In goldfish tectum, alligator cerebellum, and the CA1 field of hippocampus, field potentials likely to represent passive currents decay with time constants ranging from 4 to 10 ms (Fig. 1*c* of Andersen et al. 1978; Langdon et al. 1988b; Nicholson and Llinás 1971; Fig. 2 of Taube and Schwartzkroin 1988). The decay of W1 is considerably slower, and it is doubtful whether this could be due solely to the passive properties of the dendrites and their arbors in layers I and II. This slow decay may represent temporal dispersion of the underlying excitatory event in layer II; that is, asynchrony of excitatory postsynaptic currents in layer II, asynchronous firing by cell somata in layer II, or both.

### *Component S1: cell soma spikes evoked antidromically*

In normal medium, we observe a large, short-latency and relatively rapid negative deflection throughout much of the cortex (component S1), first distinct from the stimulus artifact in layer V and appearing to propagate upward as far as layer II at a rate of ~0.3 m/s. This pattern also appears in the depth profiles of others (Bode-Greuel et al. 1987; Shaw and Teyler 1982). We show that this component persists in media that prevent synaptic transmission. Component S1 is therefore either a "population spike" generated by the synchronous firing of neurons that send axons to the white matter, or an "afferent volley" representing the synchronous firing of axons (of extrinsic origin) ascending from the white matter. The data are most consistent with the former. There is a close resemblence in time course, amplitude, and depth distribution between S1 spikes and the synaptically driven S2 spikes that followed. The simplest explanation is that the synchronous firing of cell somata in layer III is responsible for both. The alternative is cumbersome: that component S1 is due to firing of extrinsic afferent axons (detached from their somata and synapses), but that component S2 is due to firing of some other neuronal population with its synapses intact. The reduction in component S1 by muscimol is more plausibly attributed to effects on somatic and dendritic currents than to interference with orthodromic axonal conduction. We have noted that the laminar distribution of component S1 approximates the distribution of the somata of neurons that send slowly conducting axons to the white matter. In addition, the latency of component S1 in layer III is in good accord with observations of antidromic activation of layer III pyramidal cells in rabbit visual cortex in vivo (Swadlow and Weyand 1981). Our component S1 has the same shape, amplitude, and latency of a field-potential component recorded in layer III by Gutnick and Prince (1981) in slices of guinea pig somatosensory cortex (also stimulated at the border between layer VI and white matter, and with synaptic activity suppressed with high-$Mn^{2+}$ medium). Moreover, they used intracellular recordings and dye-fills to show the presence of layer III pyramidal cells that were antidromically activated with the same latency as the $Mn^{2+}$-resistent field-potential spike. We propose that the depth profile of component S1 is that of a succession of population spikes generated with increasing latency in successively higher layers as cell somata are antidromically activated via slow-conducting efferents to the white matter.

Field potentials generated by antidromic activation of populations of pyramidal cells have been perhaps best studied in cerebellar Purkinje cells in the cat and the frog (respectively, Eccles et al. 1966; Llinás et al. 1969). Their conclusions are in general agreement with the analyses of similar data from other systems (Humphrey 1968; Rall 1977; Rall and Shepherd 1968). To summarize briefly, when a neuronal soma fires, part of the depolarizing action current flows into the dendrites, so that each dendrite participates in a current loop. In each loop, there is a leg in which current flows intradendritically, away from the cell soma, and an extracellular leg along which current returns toward the cell soma. In a pyramidal cell, the apical dendrite, compared to the others, offers the lowest resistance to current leaving the soma, so it will carry the most current and will carry it the farthest. When a neuronal field contains synchronously firing pyramidal cells with apical dendrites all oriented in parallel, the result is net extracellular current that flows parallel to the apical dendrites and toward the cell somata. This generates a field-potential dipole such as we observed, negative near the cell somata and positive toward the distal ends of the apical dendrites (cf. Llinás et al. 1969).

During the repolarizing phase of the action potential, if re- and hyperpolarizing $K^+$ conductance occurs along somatic membrane only, then the cell soma may become

more negative than the dendrites, resulting in a late reversal of the field-potential dipole (Eccles et al. 1966). We observed no such reversal after the S1 spike in $Ca^{2+}$-free medium, nor did Gutnick and Prince (1981) or Lee (1982). In the frog cerebellum, anatomic considerations leave no doubt that antidromic activation of Purkinje cells generates the population spike evoked by white matter stimulation, yet there is little or no reversing phase to the field-potential dipole (Llinás et al. 1969). Therefore the lack of such reversal does not weigh against our interpretation of S1. It does suggest that in $Ca^{2+}$-free medium, prominent $K^+$ conductances restricted to the cell soma do not occur during the repolarization phase of single firings by the neurons that generate component S1.

### *Analyses of thalamocortical transmission based on CSD profiles*

Before our work, the most detailed study of field-potential components in neocortical slices was that of by Bode-Greuel et al. (1987), who studied rat visual cortex in nearly the same manner as ourselves. Their primary data (i.e., field-potential profiles) are rather similar to ours, but their mode of analysis and interpretation differed significantly. They proposed that CSD profiles reveal a sequence beginning with postsynaptic current in layer IV at a latency of ~0.75 ms, then a longer current sink in layer III beginning at 1.5 ms, and finally a sink in layer II beginning after ~3 ms. They attributed this sequence to the serial passage of excitation through a trisynaptic pathway beginning with the thalamocortical projection to layer IV; it was thus concluded that the in vitro response to stimulation of the white matter is essentially the same as the in vivo response to stimulation (in the cat) of either the optic chiasm or the optic radiation remote from the visual cortex (Mitzdorf and Singer 1978). This interpretation of the in vitro data was based on the designation of cortex between 750 and 950 $\mu$m from the pial surface as layer IV. Our own anatomic data, that of Yamamoto and co-workers (1989), and the more detailed anatomic studies of Peters (1984) and Zilles et al. 1984 clearly show that layer IV is more superficial, spanning 550–650 $\mu$m in depth; in the rat, depths of 750 and 950 $\mu$m correspond to middle and lower layer V.

Aside from anatomic considerations, there are special problems associated with the estimation of CSDs from field potentials recorded in slices. The amplitude of a field potential depends critically on the conductivity of the extracellular medium. The conductance of saline is ~5.5 times that of neocortex, based on previous data (appendix to Mitzdorf and Singer 1980). We therefore expected a marked decrease in the amplitude of responses near the cut edges of our slices, because of this higher conductivity[2] and because of damage to neuronal elements near the edges. We clearly observed such gradients and thus conclude that some current flows along the $y$-axis. We also observed gradients oriented with the $x$-axis. Estimates of CSDs based solely on gradients along the $z$-axis thus suffer some inaccuracy and must be interpreted with caution.

[2] For a mathematical analysis of the "edge effect" due to this higher conductivity, see Klee and Rall (1977).

In the previous studies by Singer and co-workers (Bode-Greul et al. 1987; Mitzdorf and Singer 1978), it was assumed that action currents would make a negligible contribution to profiles of CSDs (based on a rationale reviewed by Mitzdorf 1985). However, our data from slices in $Ca^{2+}$-free medium and similar data from others (Gutnick and Prince 1981; Kimura et al. 1989; Lee 1982) are rather conclusive that action currents in neocortex can generate large, lamina-specific field-potential transients. Moreover, there are many examples from other preparations in which anatomic considerations leave little doubt that synchronous activation of discretely localized cell somata can produce a very large, but local, population spike (e.g., Andersen et al. 1971, 1980; Humphrey 1968; Kang et al. 1988; Llinás et al. 1969; Rall and Shepherd 1968). When second derivatives are calculated with field-potential profiles that contain such waveforms, the resulting CSD estimates will be nonzero. It follows that one cannot assume that only postsynaptic currents contribute significantly to sinks and sources observed in neocortical depth profiles.

The persistance of component S1 in layer II/III in the absence of synaptic transmission demonstrates that thalamocortical afferents to layer IV are not necessary for activation of supragranular cortex after stimulation of the white matter. Moreover, the thalamocortical projection appears to have played only a minor role in generating synaptically driven population events in layer IV, because responses in layer IV were altered very little by $Ca^{2+}$-free medium. We suggest that the slice preparation is an unlikely place to observe field-potential events directly representing pre- or postsynaptic activity in the thalamofugal projection to layer IV. If conduction velocities in the rat thalamocortical projection are comparable to those observed in the cat (20–40 m/s) (Bullier and Henry 1979), the afferent volley should be masked by the stimulus artifact. As for postsynaptic currents, the contributions of individual neurons would be likely to cancel each other because layer IV cells tend to be small and non-pyramidal in form (Gilbert 1983; Jones 1984, 1988).

### *Component S2: synaptically driven bursts of firing in layer III*

Antidromic activation was often followed by a conspicuous and stereotypic pattern of synaptically driven spike repetitions in layer III. Similar waveforms appear in previous recordings of field potentials in neocortical slices, but these were either depicted without comment (Kimura et al. 1989, their Fig. 2, *insert b*) or interpreted as due to sequential activation of different neuronal populations (Shaw and Teyler 1982, *traces 4* and *6* of their Fig. 8). Based on our single-unit data, and comparing the properties of individual S1 and S2 spikes, we see no evidence for different neuronal populations and propose rather that they are due to repeated, synchronous firing of a single neuronal population. In the following, we consider the anatomy and physiology of populations of neocortical neurons likely to be responsible for these field-potential spikes.

Based on intracellular recordings from guinea pig sensorimotor cortex, it has been proposed that there are three main physiological classes of cortical neurons: *fast-spiking*

(FS), *regular spiking* (RS), and *intrinsic bursting* (IB) cells (Chagnac-Amitai and Connors 1989b; Connors et al. 1982; McCormick et al. 1985). FS cells would not contribute to components S1 and S2 because, unlike RS and IB cells, FS neurons are thought to be inhibitory and nonpyramidal (therefore lacking direct connection with the white matter). There is a remarkable similarity between S2 spikes and the firing of IB cells injected with depolarizing current, with regards to firing frequency, burst duration, and lack of frequency adaptation. However, we think it is unlikely that S2 bursts are due to the firing of IB cells. S2 bursts depend on synaptic transmission, whereas IB cells burst intrinsically. Also, IB cells are not found in layer III.

It has also been proposed that neurons of the IB class orchestrate epileptiform activity throughout all cortical laminae via divergent interlaminar projections (Connors 1984). We do not see our studies as testing this hypothesis because of the several pronounced differences between S2 spikes and epileptiform field potentials. In our (nonepileptiform) slices, synaptically driven spikes are absent exactly where IB cells are localized: layer IV and upper layer V. This lack of a field-potential component representing IB activity could be due to any of the following: *1*) IB cells may not be fired under our conditions; *2*) when they do fire, it is not certain that their firing is phase-locked; and *3*) IB cells may not be present in sufficient density to generate an appreciable field-potential spike, because they have been encountered relatively infrequently in the intracellular studies. It remains possible, however, that IB cells fire undetected in our slices and orchestrate synchronous firing of neurons in layer III.

### *Is component S2 driven by recurrent projections of layer III neurons?*

The population bursts that we observe in layer III may be an aggregate behavior of neurons interlinked by excitatory connections, rather than because of cells that burst intrinsically (i.e., when injected with current). In many layer III pyramidal cells, single spikes elicit little or no afterhyperpolarization, and spikes are followed by a depolarizing afterpotential ~3 ms later (Chagnac-Amitai and Connors 1989b; Sutor and Hablitz 1989). These cells may thus be primed to fire again provided that excitatory synaptic input is received. Anatomic data from cats (Gilbert and Wiesel 1981; Jones 1984, 1988; Kisvardáy et al. 1986; Martin and Whitteridge 1984) and from rats (Burkhalter 1989; Feldman 1984; Paldino and Harth 1977; Parnavelas et al. 1977; Peters and Kara 1985) show that layer III pyramidal cells bear many recurrent collaterals projecting into the surrounding layer II/III. On the basis of ultrastructure and immunocytochemical evidence, these recurrent projections are thought to be excitatory (Kisvardáy et al. 1986; LeVay 1988).

Thomson et al. (1988) have presented physiological evidence that supragranular pyramidal cells are directly linked by excitatory connections. Specifically, they showed that "single-axon EPSPs" often peaked 3–4 ms after the firing of the presynaptic element. Such connections would be well suited to drive the spikes of component S2. There are similar data from studies of the CA2 and CA3 fields of rodent hippocampus (MacVicar and Dudek 1980; Miles and Wong 1986). In neocortex and in hippocampus, the data indicate that the probability of coupling between any two randomly chosen neighbors is rather low. However, synchronization of bursting may require only sparsely distributed excitatory coupling (Traub et al. 1989). We propose that the activity of any particular layer III pyramid is interdependent with the activity of certain of its neighbors with which it is linked by recurrent, short-latency excitatory connections; such neurons would thereby function conjointly as members of a cooperative "ensemble" (Fig. 16). Our horizontal profiles of response distributions and the anatomic data (Paldino and Harth 1977; Peters and

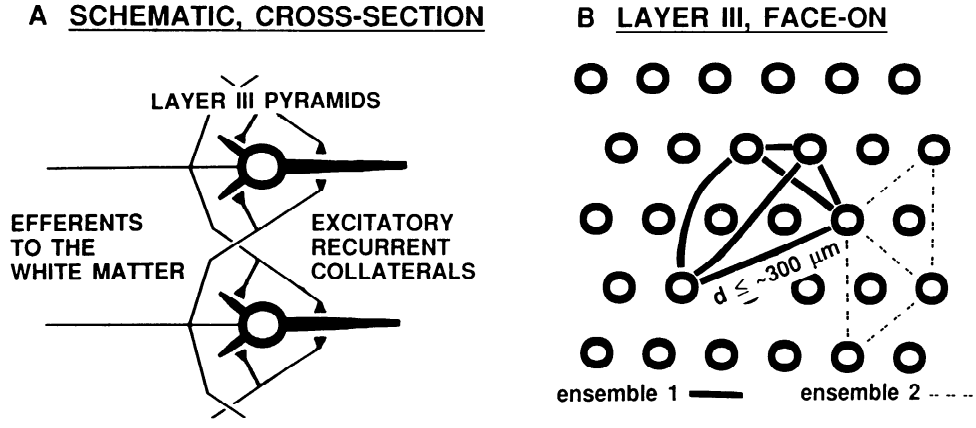


FIG. 16. Schematic depiction of the efferent axons and collaterals that we propose are responsible for synaptically driven population bursts in layer III. *A*: interconnection of layer III output neurons (pyramidal cells) via their recurrent collaterals. *B*: layer III neurons as members of ensembles; we propose that strong excitatory connections (solid and dotted lines interconnecting the "cells") may be a means whereby activity within ensembles is correlated and synchronized. Responses to features in visual space may consist of activation of specific ensembles (see text). This diagram is not intended to depict the true density of layer III pyramidal cells or layer III ensembles, nor to imply clumping or discontinuities in the density of local, horizontal projections in layer III. It is expected that many other ensembles, present but not depicted, would have territories that overlap to varying extents those of the 2 indicated.

Kara 1985) suggest that most of this short-latency excitation is delivered to neighbors within ~300 μm. Provided that the conduction velocity for these recurrent collaterals is ~0.3 m/s (as it was for the parent axons descending to the white matter), it is consistent with this hypothesis that population spikes of the same synaptic order lag by 0.3 ms for each 100 μm of horizontal displacement (Figs. 13 and 14). We propose that S2 spikes occur only when there is "spatial summation" of numerous inputs, as suggested by the greater sensitivity of component S2 (compared to S1) to proximity to the cut edges of slices (Fig. 11). In a previous study in which thinner (350 μm) slices of rat visual cortex were used (and slices were maintained in an interface-type chamber, which might further reduce the *y*-axis extent of viable slice), large S1-like waveforms were observed, but S2 spike bursts were not (Bode-Greuel et al. 1987).

By this hypothesis, far-ranging horizontal spread (Fig. 14) would result primarily from a specific form of polysynaptic transmission involving serial passage of excitation via local projections within layer III. We believe that this is the simplest explanation that fits the data, but our data do not exclude the possibility that a significant role is played by horizontal connections in other layers. Excitatory recurrent projections exist between layer V pyramidal cells (Kang et al. 1988), and, recording on beam, we often observed repeating, low-amplitude spikes in layer V (e.g., Fig. 2, 800-μm depth). Recording 1.5 mm off beam, we observed responses in layer III that began 9 ms earlier than those in the overlaying layer III. Based on anatomic data (Gilbert 1983), layer V neurons may project to supragranular neurons polysynaptically, via layers VI and IV, if not more directly. Therefore we do not dismiss the possibility that excitation spreads off beam via connections in layer V, and that after this, layer V cells off beam may either enable or drive activity in overlaying layer III.

### *Variability*

Variability between laboratories and from one preparation to the next could be due to differences in several factors, including the thickness of viable slice, the plane of slicing, the recording position, and the stimulus strength. The stimulating and recording sites are chosen blind to cortical inhomogeneities such as have been well described in cat and primate (Gilbert 1983; Gilbert and Wiesel 1981; LeVay 1988) and are also clearly present in rodent (Burkhalter 1989; Métin et al. 1988).

Our method of investigation may not produce any direct representation of inhibitory activity. We expect, however, that our responses in normal medium represent a summation of excitatory and inhibitory activities because application of disinhibitory agents greatly augments the duration and horizontal extent of cortical responses to white matter stimulation (Chagnac-Amitai and Connors 1989a; Chervin et al. 1988; Connors 1984; Langdon and Sur, unpublished observations). Synaptically driven components of field potentials thus represent, in effect, excitatory connections that have either preceded or prevailed over inhibitory activity. It remains unclear what exact conditions determine the extent to which either excitation or inhibition prevails in any particular slice maintained in normal medium.

### *Functional significance of layer III population bursts?*

Although there are several differences between component S2 and "epileptiform" field potentials (Chagnac-Amitai and Connors 1989a; Connors 1984), both present a high level of synchronization of firing and both may, at least potentially, spread horizontally at 0.05–0.1 m/s. We suspect that it may be most useful to regard epileptiform activity as a pathological phenomenon at one end of a continuum with normal function at the opposite end. In vivo, even in the absence of disinhibitory agents, electrical stimulation of the optic tract, the lateral geniculate nucleus, or the optic radiation evokes brief bursts of spike-like potentials that repeat at 300–400 Hz in supragranular visual cortex (Chang and Kaada 1950; Malis and Kruger 1956; Langdon and Sur unpublished observations). This suggests that phase-locked firing bursts in layer III may not require direct stimulation of cortex. As with frankly epileptiform activity, responses to electrical shocks applied to subcortical visual pathways or cortical columns must entail a greater synchronization of firing than would occur during normal function, but these responses may nevertheless reveal features of neocortical circuitry that play a role in the normal function of cortex.

In visual cortex, neuronal responses to visual stimuli vary as a function of cortical layer and region. Within area 17, these differences are often attributed to transformations performed as visual information passes serially through the cortical layers (Gilbert 1983; Gilbert and Wiesel 1981). Our data now suggest that there are strong, local excitatory interactions between neurons in layer III (Fig. 16). We propose, therefore, that in addition to serial arrangements, excitatory connections between elements at the same level in the information-processing chain (layer III) may also play a significant role in cortical transformations of visual information. We speculate that ensembles of layer III cells may respond selectively to specific features of visual stimuli. The output of layer III would thus be a matter of which ensembles (rather than which individual neurons) were active at any time. With the output of an ensemble determined conjointly by its constituent neurons, there would be a more decisive response once the level of specific stimulation had reached a threshold. The concerted output of an entire ensemble acting together would be better able to orchestrate and synchronize activity in other cortical regions, and this may play a role in identifying local features that are part of a more global stimulus pattern (Gray and Singer 1989[3]). Concerning the ability of neuronal circuits to organize themselves, various data suggest that temporal correlation of activity plays an important role in the devel-

[3] Gray and co-workers have recently reported (Gray et al. 1989; Gray and Singer 1989) a different kind of synchronization of neuronal activity in visual cortex that should not be equated with the phase-locked burst firing that we describe. Specifically, they report that single units in cat visual cortex in vivo oscillate in synchrony between rapid and slow rates of firing while responding to visual stimulation. These oscillations are regular, with firing rate maxima occurring every 20–40 ms. In contrast, we describe synchronization of the firing of *individual spikes*, with these spikes repeating at 3- to 4-ms intervals for ~15 ms. These phenomena may be unrelated, but it is also possible that high-frequency bursts such as we observe in layer III repeat at 20- to 40-ms intervals during visual activity to contribute to the oscillations described by Gray et al. (1989).

opment and/or maintenance of useful order in neuronal connections. It is plausible that synchronization of firing within output ensembles of primary visual cortex is a means by which projections are ordered in its target fields.

M. Esguerra played a significant role in preliminary aspects of this investigation and in discussions of the data. D. Kuhn provided excellent assistance during a significant portion of the data collection.

This work was supported by National Eye Institute Grant EY-07023.

Address for reprint requests: R. B. Langdon, Dept. of Behavioral Neuroscience, 446 Crawford Hall, University of Pittsburgh, Pittsburgh, PA 15260.

Received 4 October 1989; accepted in final form 19 June 1990.

## REFERENCES

ALGER, B. E., DHANJAL, S. S., DINGLEDINE, R., GARTHWAITE, J., HENDERSON, G., KING, G. L., LIPTON, P., NORTH, A., SCHWARTZKROIN, P. A., SEARS, T. A., SEGAL, M., WHITTINGHAM, T. S., AND WILLIAMS, J. Brain slice methods. In: *Brain Slices,* edited by R. Dingledine. New York: Plenum, 1984, p. 381–437.

ANDERSEN, P., BLISS, T. V. P., AND SKREDE, K. K. Unit analysis of hippocampal population spikes. *Exp. Brain Res.* 13: 208–221, 1971.

ANDERSEN, P., SILFVENIUS, H., SUNDBERG, S. H., AND SVEEN, O. A comparison of distal and proximal dendritic synapses on CA1 pyramids in guinea-pig hippocampal slices in vitro. *J. Physiol. Lond.* 307: 273–299, 1980.

ANDERSEN, P., SILFVENIUS, H., SUNDBERG, S. H., SVEEN, O., AND WIGSTRÖM. Functional characteristics of unmyelinated fibers in the hippocampal cortex. *Brain Res.* 144: 11–18, 1978.

ARTOLA, A. AND SINGER, W. Long-term potentiation and NMDA receptors in rat visual cortex. *Science Wash. DC* 330: 649–652, 1987.

BODE-GREUEL, K. M., SINGER, W., AND ALDENHOFF, J. B. A current source density analysis of field potentials evoked in slices of visual cortex. *Exp. Brain Res.* 69: 213–219, 1987.

BULLIER, J. AND HENRY, G. H. Ordinal position of neurons in cat striate cortex. *J. Neurophysiol.* 42: 1251–1263, 1979.

BURKHALTER, A. Intrinsic connections of rat primary visual cortex: laminar organization of axonal projections. *J. Comp. Neurol.* 279: 171–186, 1989.

BURNE, R. A., PARNAVELAS, J. G., AND LIN, C.-S. Response properties of neurons in the visual cortex of the rat. *Exp. Brain Res.* 53: 374–383, 1984.

CHAGNAC-AMITAI, Y. AND CONNORS, B. W. Horizontal spread of synchronized activity in neocortex and its control by GABA-mediated inhibition. *J. Neurophysiol.* 61: 747–758, 1989a.

CHAGNAC-AMITAI, Y. AND CONNORS, B. W. Synchronized excitation and inhibition driven by intrinsically bursting neurons in neocortex. *J. Neurophysiol.* 62: 1149–1162, 1989b.

CHANG, H.-T. AND KAADA, B. An analysis of primary response of visual cortex to optic nerve stimulation in cats. *J. Neurophysiol.* 13: 305–318, 1950.

CHERVIN, R. D., PIERCE, P. A., AND CONNORS, B. W. Periodicity and directionality in the propagation of epileptiform discharges across neocortex. *J. Neurophysiol.* 60: 1695–1713, 1988.

CONNORS, B. W. Initiation of synchronized neuronal bursting in neocortex. *Nature Lond.* 310: 685–687, 1984.

CONNORS, B. W., GUTNICK, M. J., AND PRINCE, D. A. Electrophysiological properties of neocortical neurons in vitro. *J. Neurophysiol.* 48: 1302–1320, 1982.

DINGLEDINE, R. AND SOMJEN, G. Calcium dependence of synaptic transmission in the hippocampal slice. *Brain Res.* 207: 218–222, 1981.

ECCLES, J. C., KATZ, B., AND KUFFLER, S. W. Nature of the "endplate potential" in curarized muscle. *J. Neurophysiol.* 4: 362–387, 1941.

ECCLES, J. C., LLINÁS, R., AND SASAKI, K. The action of antidromic impulses on the cerebellar Purkinje cells. *J. Physiol. Lond.* 182: 316–345, 1966.

FELDMAN, M. L. Morphology of the neocortical pyramidal neuron. In: *Cerebral Cortex: Cellular Components of the Cerebral Cortex,* edited by A. Peters and E. G. Jones. New York: Academic, 1984, vol. 1, p. 123–200.

FREEMAN, J. A., SCHMIDT, J. T., AND OSWALD, R. E. Effect of $\alpha$-bungarotoxin on retinotectal synaptic transmission in the goldfish and the toad. *Neuroscience* 5: 929–942, 1980.

FRÉGNAC, Y. AND IMBERT, M. Development of neural selectivity in primary visual cortex of cat. *Physiol. Rev.* 64: 325–434, 1984.

GILBERT, C. D. Microcircuitry of the visual cortex. *Annu. Rev. Neurosci.* 6: 217–247, 1983.

GILBERT, C. D. AND WIESEL, T. N. Laminar specialization and intracortical connections in cat primary visual cortex. In: *The Organization of Cerebral Cortex,* edited by F. O. Schmidt, F. G. Worden, G. Adelman, and S. G. Dennis. Cambridge, MA: MIT Press, 1981, p. 163–191.

GRAY, C. M., KÖNIG, P., ENGEL, A. K., AND SINGER, W. Oscillatory responses in cat visual cortex exhibit inter-columnar synchronization which reflects global stimulus properties. *Nature Lond.* 338: 334–337, 1989.

GRAY, C. M. AND SINGER, W. Stimulus-specific oscillations in orientation columns in cat visual cortex. *Proc. Natl. Acad. Sci. USA* 86: 1698–1702, 1989.

GUTNICK, M. J. AND PRINCE, D. A. Dye coupling and possible electrotonic coupling in the Guinea pig neocortical slice. *Science Wash. DC* 211: 67–70, 1981.

HABERLY, L. B. AND SHEPHERD, G. M. Current-density analysis of summed evoked potentials in opossum prepyriform cortex. *J. Neurophysiol.* 36: 789–802, 1973.

HACKETT, J. T. Calcium dependency of excitatory chemical synaptic transmission in the frog cerebellum in vitro. *Brain Res.* 114: 35–46, 1976.

HAMASAKI, T., KOMATSU, Y., YAMAMOTO, N., NAKAJIMA, S., HIRAKAWA, K., AND TOYAMA, K. Electrophysiological study of synaptic connections between a transplanted lateral geniculate nucleus and the visual cortex of the host rat. *Brain Res.* 422: 172–177, 1987.

HUBEL, D. H. Exploration of the primary visual cortex, 1955–1978. *Nature Lond.* 299: 515–524, 1982.

HUMPHREY, D. R. Re-analysis of the antidromic cortical response. II. On the contribution of cell discharge and PSPs to the evoked potentials. *Electroencephalogr. Clin. Neurophysiol.* 24: 116–129, 1968.

JONES, E. G. Laminar distribution of cortical efferent cells. In: *Cerebral Cortex: Cellular Components of the Cerebral Cortex,* edited by A. Peters and E. G. Jones. New York: Academic, 1984, vol. 1, p. 521–553.

JONES, E. G. What are the local circuits? In: *Neurobiology of Neocortex,* edited by P. Rakic and W. Singer. New York: Wiley, 1988, p. 137–152.

KANG, Y., ENDO, K., AND ARAKI, T. Excitatory synaptic actions between pairs of neighboring pyramidal tract cells in the motor cortex. *J. Neurophysiol.* 59: 636–647, 1988.

KATZ, B. *The Release of Neurotransmitter Substances.* Liverpool, UK: Liverpool Univ. Press, 1969.

KIMURA, F., NISHIGORI, A., SHIROKAWA, T., AND TSUMOTO, T. Long-term potentiation and *N*-methyl-D-aspartate receptors in the visual cortex of young rats. *J. Physiol. Lond.* 414: 125–144, 1989.

KISVARDÁY, Z. F., MARTIN, K. A. C., FREUND, T. F., MAGLÓCZKY, ZS., WHITTERIDGE, D., AND SOMOGYI, P. Synaptic targets of HRP-filled layer III pyramidal cells in the cat striate cortex. *Exp. Brain Res.* 64: 541–552, 1986.

KLEE, M. AND RALL, W. Computed potentials of cortically arranged populations of neurons. *J. Neurophysiol.* 40: 647–666, 1977.

KRNJEVIĆ, K. Chemical nature of synaptic transmission in vertebrates. *Physiol. Rev.* 54: 418–540, 1974.

KOMATSU, Y., FUJII, K., MAEDA, J., SAKAGUCHI, H., AND TOYAMA, K. Long-term potentiation of synaptic transmission in kitten visual cortex. *J. Neurophysiol.* 59: 124–141, 1988.

LANGDON, R. B., ESGUERRA, M., AND SUR, M. Transmission events in mammalian visual cortex that involve NMDA and non-NMDA glutamate receptors. *Soc. Neurosci. Abstr.* 14: 200, 1988a.

LANGDON, R. B. AND FREEMAN, J. A. Pharmacology of retinotectal transmission in the goldfish: effects of nicotinic ligands, strychnine, and kynurenic acid. *J. Neurosci.* 7: 760–773, 1987.

LANGDON, R. B. AND JACOBS, R. S. An inexpensive frequency-modulated (FM) audio monitor of time-dependent analog parameters. *J. Pharmacol. Methods* 3: 181–190, 1980.

LANGDON, R. B., KUHN, D. M., AND SUR, M. Synchronous, coherent burst-firing by neurons in lamina III of rat visual cortex in vitro. *Soc. Neurosci. Abstr.* 15: 797, 1989.

LANGDON, R. B., MANIS, P. B., AND FREEMAN, J. A. Goldfish retinotectal transmission in vitro: component current sink-source pairs isolated by varying calcium and magnesium levels. *Brain Res.* 441: 299–308, 1988b.

LEE, K. S. Sustained enhancement of evoked potentials following brief,

high-frequency stimulation of the cerebral cortex in vitro. *Brain Res.* 239: 617–623, 1982.

LEVAY, S. Patchy intrinsic projections in visual cortex, area 18, of the cat: morphological and immunocytochemical evidence for an excitatory function. *J. Comp. Neurol.* 269: 265–274, 1988.

LLINÁS, R., BLOEDEL, J. R., AND HILLMAN, D. E. Antidromic invasion of Purkinje cells in frog cerebellum. *J. Neurophysiol.* 32: 881–891, 1969.

LLINÁS, R. AND NICHOLSON, C. Analysis of field potentials in the central nervous system. In: *Handbook of Electroencephalography and Clinical Neurophysiology,* edited by C. F. Stevens. Amsterdam: Elsevier, 1974, vol. 2, part B, p. 61–83.

LORENTE DE NÓ, R. Action potential of the motoneurons of the hypoglossus nucleus. *J. Cell. Comp. Physiol.* 29: 207–287, 1947.

LUND, J. S. Intrinsic organization of the primate visual cortex, area 17, as seen in Golgi preparations. In: *The Organization of Cerebral Cortex,* edited by F. O. Schmidt, F. G. Worden, G. Adelman, and S. G. Dennis. Cambridge, MA: MIT Press, 1981, p. 105–124.

MACVICAR, B. A. AND DUDEK, F. E. Local synaptic circuits in rat hippocampus: interactions between pyramidal cells. *Brain Res.* 184: 220–223, 1980.

MALIS, L. I. AND KRUGER, L. Multiple response and excitability of cat's visual cortex. *J. Neurophysiol.* 19: 172–186, 1956.

MARTIN, K. A. C. AND WHITTERIDGE, D. Form, function and intracortical projections of spiny neurones in the striate visual cortex of the cat. *J. Physiol. Lond.* 353: 463–504, 1984.

MCCORMICK, D. A., CONNORS, B. W., LIGHTHALL, J. W., AND PRINCE, D. A. Comparative electrophysiology of pyramidal and sparsely spiny stellate neurons of the neocortex. *J. Neurophysiol.* 54: 782–806, 1985.

MÉTIN, C., GODEMENT, P., AND IMBERT, M. The primary visual cortex in the mouse: receptive field properties and functional organization. *Exp. Brain Res.* 69: 594–612, 1988.

MILES, R. AND WONG, R. K. S. Excitatory synaptic interactions between CA3 neurones in the guinea-pig hippocampus. *J. Physiol. Lond.* 373: 397–418, 1986.

MITZDORF, U. Current source-density method and application in cat cerebral cortex: investigation of evoked potentials and EEG phenomena. *Physiol. Rev.* 65: 37–100, 1985.

MITZDORF, U. AND SINGER, W. Prominent excitatory pathways in the cat visual cortex (A17 and A18): a current source density analysis of electrically evoked potentials. *Exp. Brain Res.* 33: 371–394, 1978.

MITZDORF, U. AND SINGER, W. Monocular activation of visual cortex in normal and monocularly deprived cats: an analysis of evoked potentials. *J. Physiol. Lond.* 304: 203–220, 1980.

NICHOLSON, C. AND FREEMAN, J. A. Theory of current source-density analysis and determination of conductivity tensor for anuran cerebellum. *J. Neurophysiol.* 38: 356–368, 1975.

NICHOLSON, C. AND LLINÁS, R. Field potentials in the alligator cerebellum and theory of their relationship to Purkinje cell dendritic spikes. *J. Neurophysiol.* 34: 509–531, 1971.

PALDINO, A. AND HARTH, E. A computerized study of Golgi-impregnated axons in rat visual cortex. In: *Computer Analysis of Neuronal Structures,* edited by R. D. Lindsey. New York: Plenum, 1977, p. 189–207.

PARNAVELAS, J. G., LIEBERMAN, A. R., AND WEBSTER, K. E. Organization of neurons in the visual cortex, area 17, of the rat. *J. Anat.* 124: 305–322, 1977.

PAXINOS, G. AND WATSON, C. *The Rat Brain in Stereotaxic Coordinates* (2nd ed.). New York: Academic, 1986.

PERKINS, A. T., IV AND TEYLER, T. J. A critical period for long-term potentiation in the developing rat visual cortex. *Brain Res.* 439: 222–229, 1988.

PETERS, A. The visual cortex of the rat. In: *Cerebral Cortex: Visual Cortex,* edited by A. Peters and E. G. Jones. New York: Plenum, 1984, vol. 3, p. 19–80.

PETERS, A. AND KARA, D. A. The neuronal composition of area 17 of rat visual cortex. I. The pyramidal cells. *J. Comp. Neurol.* 234: 218–241, 1985.

RALL, W. Time constants and electrotonic length of membrane cylinders and neurons. *Biophys. J.* 9: 1483–1508, 1969.

RALL, W. Core conductor theory and cable properties of neurons. In: *Handbook of Physiology. The Nervous System. Cellular Biology of Neurons.* Betheseda, MD: Am. Physiol. Soc., 1977, sect. 1, vol. I, pt. 1, p. 39–97.

RALL, W. AND SHEPHERD, G. M. Theoretical reconstruction of field potentials and dendrodendritic synaptic interactions in olfactory bulb. *J. Neurophysiol.* 31: 884–915, 1968.

RICHARDS, C. D. AND SERCOMBE, R. Calcium, magnesium and electrical activity of the guinea pig olfactory cortex in vitro. *J. Physiol. Lond.* 211: 571–584, 1970.

SHAW, C. AND TEYLER, T. J. The neural circuitry of the neocortex examined in the in vitro brain slice preparation. *Brain Res.* 243: 35–47, 1982.

SHERMAN, S. M. AND SPEAR, P. D. Organization of visual pathways in normal and visually deprived cat. *Physiol. Rev.* 62: 738–855, 1982.

SUTOR, B. AND HABLITZ, J. J. EPSPs in rat neocortical neurons in vitro. I. Electrophysiological evidence for two distinct EPSPs. *J. Neurophysiol.* 61: 607–620, 1989.

SWADLOW, H. A. AND WEYAND, T. G. Efferent systems of the rabbit visual cortex: laminar distribution of the cells of origin, axonal conduction velocities, and identification of axonal branches. *J. Comp. Neurol.* 203: 799–822, 1981.

TAUBE, J. S. AND SCHWARTZKROIN, P. A. Mechanisms of long-term potentiation: a current-source density analysis. *J. Neurosci.* 8: 1645–1655, 1988.

THOMSON, A. M., GIRDLESTONE, D., AND WEST, D. C. Voltage-dependent currents prolong single-axon postsynaptic potentials in layer III pyramidal neurons in rat neocortical slices. *J. Neurophysiol.* 60: 1896–1907, 1988.

TRAUB, R. D., MILES, R., AND WONG, R. K. S. Model of the origin of rhythmic population oscillations in the hippocampal slice. *Science Wash. DC* 243: 1319–1325, 1989.

YAMAMOTO, N., KUROTANI, T., AND TOYAMA, K. Neural connections between the lateral geniculate nucleus and visual cortex in vitro. *Science Wash. DC* 245: 192–194, 1989.

ZILLES, K. *The Cortex of the Rat: A Stereotaxic Atlas.* Berlin: Springer-Verlag, 1985.

ZILLES, K., WREE, A., SCHLEICHER, A., DIVAC, I. The monocular and binocular subfields of the rat's primary visual cortex. A quantitative approach. *J. Comp. Neurol.* 226: 391–402, 1984.